SCUOLA DI DOTTORATO
UNIVERSITÀ DEGLI STUDI DI MILANO-BICOCCA

School of Medicine and Surgery

PhD program in Neuroscience

Cycle XXIX

MUSCLE COORDINATION IN THE FEED-FORWARD CONTROL OF POSTURE

Surname Piscitelli

Name Daniele

Registration number 787788

Tutor: Prof. Cesare G. Cerri

Coordinator: Prof. Guido A. Cavaletti

ACADEMIC YEAR 2015/2016

"Gravity explains the motions of the planets,
but it cannot explain who sets the planets in motion."
Sir Isaac Newton

ACKNOWLEDGMENTS

I would to express my gratitude and thanks to my advisor Prof. Cesare G. Cerri for the continuous support of my Ph.D. project as well as the other research activities carried out during the last three years. I also express my warmest gratitude to Dr. Roberto Meroni, who encouraged and supported me, making my Ph.D. experience productive and stimulating.

I am deeply grateful to Prof. Mark L. Latash. From the beginning, during my year at Penn State University, he always encouraged and supported my project allowing me to grow as a research scientist. Without his continuous guidance, enthusiasm and knowledge this study would hardly have been completed.

I also extend my gratitude to all members of Motor Control Laboratory at Penn State: Ali Falaki, Stanislaw Solnik, Hang Jin Jo, Mu Qiao, Tao Zhou, Satyajit Ambike, Sasha Reschechtko, Daniela Mattos, Behnoosh Parsa, and Visiting Scholars: Omid Rasouli, Mariusz Furmanek, and Fariba Barani. They have been not only wonderful colleague but also great friends.

My permanence in State College has been a unique experience, I'm grateful to my roommate, Lorna and all the people I had the opportunity of meeting, everyone has a special place in my memories. Also, I thank my friends in Italy.

I would also like to thank my family for the invaluable help and support they provided me through my entire life.

Lastly, and most importantly I would like to thank my wife Sara, she has been and she is my Inspiration. “Doce ergo me suavitatem inspirando caritatem ... Doce me disciplinam donando patientiam, doce me scientiam illuminando intelligentiam.

S. Agostino (En. in ps. 118, 17, 4)”.

Daniele

TABLE OF CONTENTS

LIST OF TABLES

LIST OF FIGURES

ABSTRACT

The framework of the uncontrolled manifold (UCM) hypothesis has been used to study a type of feed-forward postural adjustments anticipatory synergy adjustments (ASAs) compared to anticipatory postural adjustments (APAs). ASAs reflect attenuation of a synergy index stabilizing a variable (e.g., center of pressure anterior-posterior coordinate, COP_{AP}) in preparation to a quick change in that variable, while APAs are the means of generating net forces and moments of force that minimize the effects of a predictable perturbation on posture. ASAs and APAs were explored in preparation to a self-triggered postural perturbation in conditions when the direction of the perturbation was known and unknown.

Eleven healthy subjects stood on a force platform and performed two tasks: (1) voluntary cyclic body sway in the anterior-posterior (AP) direction at 0.5 Hz; and (2) self-paced load release task in two conditions where the perturbation direction was either known or unknown (randomized by the experimenter). Surface electromyograms of 13 leg and trunk muscles as well as COP_{AP} displacements were recorded and analyzed. The first task was used to identify four muscle modes (M-modes, muscle groups with parallel scaling of activation levels). Further, inter-trial variance in the M-mode space was quantified within the UCM and orthogonal (ORT) space. An index of synergy (ΔV) was computed reflecting the relative amount of inter-trial M-mode variance within the UCM for COP_{AP}.

The index of multi-M-mode synergies showed a drop starting about 200 ms prior to the time of perturbation. These ASAs were similar across conditions. In

contrast, the timing and structure of APAs differed depended on knowledge of the perturbation direction. Namely, APAs were delayed when the perturbation direction was unknown. In addition, analysis of co-activation and reciprocal activation within agonist–antagonist muscle pairs showed predominance of reciprocal patterns in conditions when the subjects knew the perturbation direction and co- activation patterns when the perturbation direction was unknown.

The results demonstrate the existence of two separate mechanisms of feed-forward control of vertical posture. These findings potentially have implication for elucidating impaired postural control in neurological and musculoskeletal disorders and being incorporated in rehabilitation strategies.

1 INTRODUCTION

1.1 Motor control theories

Motor control is a growing field of natural science aiming at explore how the nervous system interacts with other body parts and the environment to produce purposeful, coordinated actions (Latash **2012**). It is a promising area with strong implication in the understanding motor impairments and development of specific strategies (Piscitelli **2016**).

Currently, two theories of motor control have been developed in the last decades, one approach fits the idea that the central nervous system (CNS) performs computations and specifications of motor output i.e., Electromyographic (EMG) patterns in order to achieve a desired action. The second one is based on a physical approach in which forces and motion are not pre-programmed but emerged as a consequence of shifts in the equilibrium state, that the organism and the environment tend to achieve within process of the reciprocal interaction (Feldman and Levin **2009;** Latash **2016b**).

1.1.1 Computational approach

This approach has been addressed as "internal models" and "motor program" (reviewed in Schmidt **1975;** Kawato **1999**). Briefly, according to this framework two classical control schemes have been elaborated: direct and inverse models. Within direct models the CNS compute each variable of the movement modelling causal relationship between actions and their consequences, e.g., a direct model of a

reaching task combines the actual state of the arm (velocity, position), and the actual input to predict the future state of the arm (velocity, position). The principal feature of these models is to predict the behavior of the body and environment, indeed some authors (reviewed in Wolpert and Ghahramani **2000**) use the terms 'Internal', 'predictors' and 'forward models' as synonymous.

On the other hand, inverse models are based upon opposite transformations, from desired consequences to corresponding actions. In this framework to perform an action as a pointing task the CNS has to build a motor program to translate the desired trajectory (time profiles of forces) into appropriate inputs (computed by the brain and realized by the muscles) to drive the arm along that planned trajectory. Moreover, direct and inverse model have been associated in a single scheme allowing to predict and perform movement with high accuracy (Shadmehr and Wise **2005**). Therefore, computational approaches share the idea that somewhere in the CNS networks there is a pre-computation of each variable that allow to perform a motor action. In **Figure 1.1** is illustrated a structure of the main steps involved to perform a pointing task from a starting position $\{X_{start}\}$ to a certain final position $\{X_{target}\}$ according to direct and inverse model (Latash and Zatsiorsky **2015**).

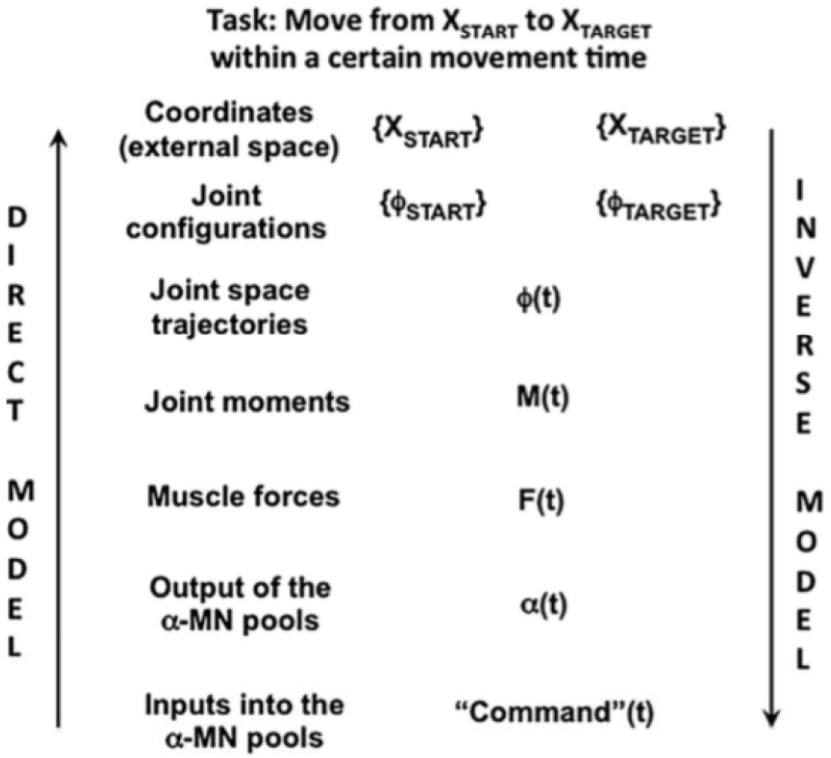

Figure 1.1: A scheme of the main steps involved in movement production of a voluntary movement. From Latash and Zatsiorsky (**2015**)

Internal models arise several issues that the CNS need to solve:

1) accurate prediction of movement kinematics, including time profiles of muscle length, velocity, and force, is necessary prior to movement initiation.
2) the steps involved require computation of signals based on a smaller set of inputs, that is, solving problems of motor redundancy.
3) time delay of signal transmission within the nervous system, from the brain to the effectors and from the peripheral sensors to the brain. Moreover, there is to take into account the relatively slow force production by the skeletal muscles.

1.1.2 Physical-based approach

The second main theory on motor control consider the CNS not as a computational system but a physical one (Latash **2010**). Within this framework, motor control is defined as a subfield of the physical approach to biological movement, searching for laws of nature describing interactions within the body and between the body and the environment that lead to natural movements (Latash **2012**). From this point of view, physical laws of nature that control the whole chemical, mechanical, and physiological processes become the starting point to understand behavior of biological systems. Some of the laws may be unknown at this time, e.g., those related to such notions as intentionality, while other are well established. In particular laws of classical mechanics can be used to describe the behavior of inanimate objects. For example, Newton's law of universal gravitation states that every two particles M_1 and M_2 attract one another with a force (F) that is proportional to the product of their masses and inversely proportional to the square of the distance between them (R^2). No force computation is required, but forces will emerge by the interactions of the two objects, following the law of gravity. This universal physical law links the state of objects with the help of parameters that describe salient proprieties of those objects.

Although living system do not violate any basic physical laws, they differ from inanimate objects, in a such way that their behavior cannot be predicted based on those laws and their actions are constrained rather than predefined by these laws (Zatsiorsky et al. **2005**). Indeed, if one knows the forces acting on an inanimate object and his initial state, its behavior can be predicted by means of classical mechanics'

laws. On the contrary, the behavior of living system cannot be predicted based on the knowledge of its initial state and salient parameters (e.g., mass).

Following this framework, it is possible to develop a new definition of living systems that goes beyond the simple description of their features such as metabolism, adaptation, growth, homeostasis, self-organization and some others. A living system is a system able to: (1) unite basic physical laws into chains and clusters leading to new stable and pervasive relations among physical variables and involving new parameters; and (2) modify these parameters in a purposeful way (Latash **2016a**, **2016b**). This definition implies that new physical laws emerge in living system and they are able to modify parameters of those new laws in a purposeful way to achieve their goals.

Since the outcomes of motor elements (e.g., movement trajectories, muscle forces and torques) involved in action are function of time, biological actions may be considered outputs of dynamical systems (Kelso **1995**) and cannot be prescribed by any neural controller. Moreover, the actual conditions of the environment are characterized by non-predictable changes. In this context, the behavior of dynamical systems can be controlled and modified by changing parameters that belong to that system (Glansdorf and Prigogine **1971**), consequently their output emerges according to the laws of physics and the interaction with the environment. Parameters do not influence the nature of physical law but play a key role on their outcomes. In the example mentioned above about Newton's law of universal gravitation, mass of the objects is a parameter that governs the attracting force between the two particles. Parameters can be classified in two subsets (Feldman **2015**): 1) one consists of parameters constrained by physical laws, e.g., gravitational constant, speed of light. 2)

the other subset consists of constant and variables that are not law-constrained. Such parameters can be modified by living systems and are addressed as control variables. For example, if one consider a pendulum - a weight suspended from a pivot, some parameters that defined its motion i.e., masses of the weight, length of the rod and the coordinates of its suspension point are not constrained by the law of gravity. Those parameters can be changed leading to a modification of the pendulum motion in time and/or in space while the force of gravity remain constant. This approach to motor control, considering living systems active rather than reactive and the idea that they can change their internal state finds its roots about half a century ago (Bernstein **1967**).

According to this framework, two main related aspects of motor control have been developed. One is based on parametric control to produce movement, the other one relates to stability of motor action and to the problem of motor redundancy (Bernstein **1967**). Furthermore, there have been several efforts to merge these two aspects into a single theory of motor control based on a multi-level scheme of hierarchical control of motor action (Latash **2010;** Latash and Huang **2015**).

1.2 The equilibrium-point hypothesis

According to the equilibrium-point (EP) hypothesis (Feldman **1966**, **1986**) developed about 50 years ago, the CNS controls movements by manipulating the threshold muscle length (λ) at which muscles begin to be activated. Initially, the EP theory was related to the control of a simple one degree-of-freedom joint, then gradually the hypothesis addressed more complex movements and actions within multi-joint systems, such as locomotion, sit-to-stand and reaching, combining motor

action with perception (Feldman **2015**, **2016**). Since the time of its formulation EP hypothesis has been addressed as referent configuration hypothesis (Feldman and Levin **1995**) and threshold control hypothesis (Feldman **2011**).

Parametric control of motor action has empirically been identified in a series of experiments in humans (Asatryan and Feldman **1965;** reviewed in Feldman **2015**), comparing involuntary arm movements elicited by sudden unloading of preloaded muscles (i.e., the unloading reflex) with both intentional arm movements produced by subjects and passive arm motion made by the experimenter.

In the unloading experiment subjects were asked to place the forearm on a horizontal manipulandum and held a handle, while EMG activity of biceps and triceps brachii muscles and forearm torque and position were recorded. To create an initial torque loads were connected on the manipulandum by pulleys and small electromagnetic locks. Participants established a certain initial angle counteracting the torque applied to the manipulandum. The combination of torque and elbow angle was defined as the initial equilibrium point (EP). The initial position was shown as a dot on a feedback screen placed in front of subjects. Once the initial EP (**Figure 1.2**, filled dots) was established, the load was suddenly removed while subjects were instructed to close their eyes and not to intervene voluntarily. This resulted in an involuntary motion of the forearm to another torque-angle combination, a new EP (**Figure 1.2**, open dots). Then in each trial the initial load was restored and the unloading was repeated with the same or a different load, leading to various final EPs. All the EPs form the same initial EP described a mono-tonic nonlinear torque-angle curve (**Figure**

1.2, solid curves). In the context of dynamical systems theory, the EPs can be considered as point attractors (Feldman **2015**).

The series was repeated asking subjects to intentionally change the initial position, compensating another load torque with a different elbow angle. Subsequently, the unloading procedure was repeated with a new initial EP. This resulted in a shift in the torque-angle characteristics. These family of curves were called invariant characteristics (ICs). Mathematically, each of this curve represents a one-dimensional set of EPs and each individual curve crosses a straight line drawn through it at a different point. Moreover, different ICs were separated in the angular space, highlighting that the shifts resulted from changes in a parameter having a spatial (angular) dimension.

An additional torque-angle characteristic was recorded by slow passive rotation in the whole biomechanical range of the manipulandum with the forearm on it while the subject was asked to fully relax arm muscles (‘‘passive-torque-angle characteristic’’; **Figure 1.2**, dashed curve). The ICs merged with the passive joint characteristic at different angles. These bifurcation points indicate the specific joint angles at which elbow flexors (**Figure 1.2**, upper panel) or extensor (**Figure 1.2**, lower panel) began to generate active muscle torque. The threshold angles were different for different unloading characteristics. Namely, intentional transition from one initial EP to another (voluntary movement) was elicited by shifts in the threshold angular position (R) at which the elbow muscles began to generate active torque. In other words, each threshld angle (R) corresponds to the threshold lengths (λ) at which muscles begin to be recruited. **Figure 1.2** also shows that muscle exhibits larger torques for larger

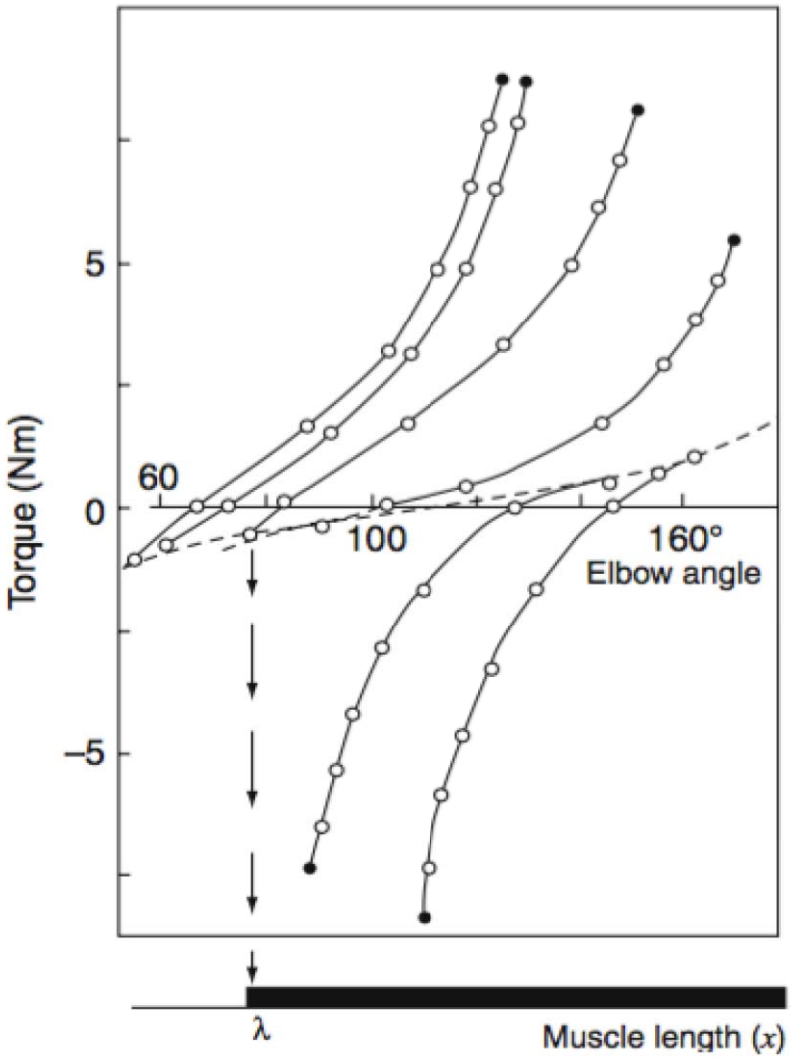

Figure 1.2: A family of static torque-angle characteristics (solid curves) obtained in unloading experiments. Each of the filled circles shows the respective mean initial combination (EP) of the joint angle and torque established by the subject before unloading. Open circles show the combinations of the same variables (final EPs) established after unloading. The dashed curve shows the passive torque-angle characteristic. From Feldman and Levin (**2009**)

deviations of its length from λ. The experiment revealed that the intentional movement was produced by a shift of λ. In other words, the CNS by setting spatial threshold controls movements. These parameters (R and λ) are settled in advance of

changes in the EMGs patterns, muscle forces, and kinematics. According to this framework, movements are not controlled by means of preprogramming motor commands, but depend on the specification of λ and external conditions.

Previously, central control of the threshold muscle length (λ) at which muscles begin to be recruited was described by Matthews (**1959**) who studied the characteristics of the tonic stretch reflex of the leg muscles in decerebrated cats. In the experiment, Matthews (**1959**) documented that the relation of tension-extension of the Soleus muscle can be changed by modifying the activity of muscles spindles by means of anesthesia of axons of γ–motoneurons. The threshold of the tonic stretch reflex increased when γ–motoneurons were progressively blocked (**Figure 1.3**, lower panel), leading to a shift of the tension-extension characteristic from its initial position (**Figure 1.3**, upper panel).

Furthermore, Matthews (**1959**) not only showed the spatial threshold can be influenced from changes in γ-afferents but also by heteronymous reflexes e.g. crossed-extensor facilitation or reciprocal inhibition between agonist and antagonist α-motoneurons. These results showing that the muscle length, λ, at which muscles begin to be recruited is primarily controlled by the CNS can be considered as a precursor of the EP hypothesis (Feldman **2015**).

The central setting of spatial threshold of muscles activation was supported and confirmed in a later study (Feldman and Orlovsky **1972**). In this experiment authors not only reproduced the previous Matthews' results but also showed that several

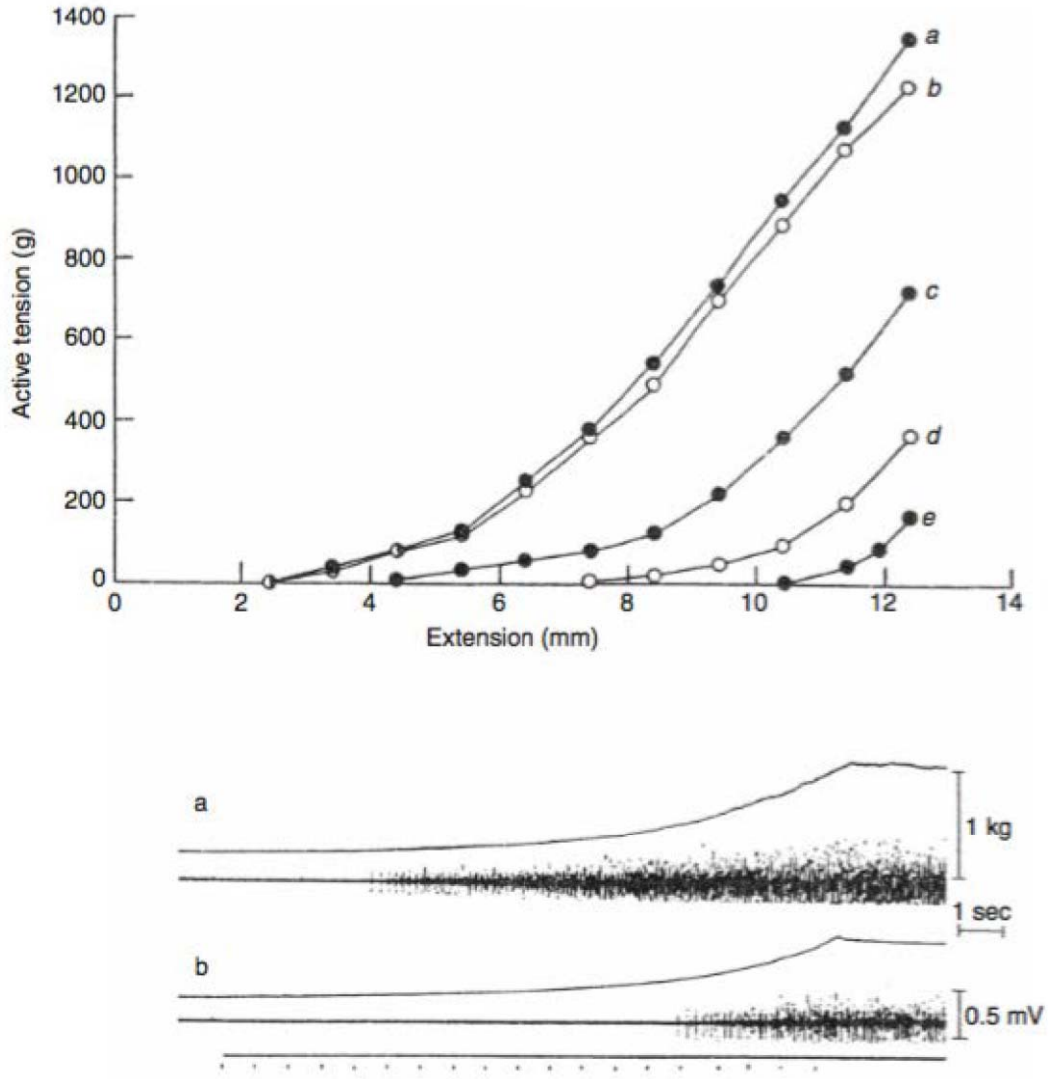

Figure 1.3: In the upper panel, an increase in the reflex threshold of the soleus-gastrocnemius muscles in the decerebrated cat is illustrated by shifts of the tension-extension curve from initial position a to the right (b–e) when the γ -fibers in the muscle nerve are progressively blocked by an anesthetic. In the lower panel, the same effect is illustrated by showing that a greater lengthening of the muscles is required to evoke EMG activity in the muscles when γ -fibers are blocked (lower traces, compare with upper traces obtained without anesthesia). From Matthews (**1959**)

descending systems (i.e., the reticulo- vestibulo- and rubro-spinal systems) have the capacity to influence the activation threshold length. Moreover, recent data (Krawitz

et al. **2001;** Fedirchuk and Dai **2004;** Heckman et al. **2008**) suggest that inputs from the brainstem can modify electric threshold of α-motoneurons and might be considered an additional mechanism of the control of threshold muscle length. Indeed, Fedirchuk and Dai (**2004**) shown that descending pathways from the brainstem can increase the membrane potential of motoneurons, resulting in a decrease of the electrical threshold at which the neuron is recruited, leading to a shift in the threshold muscle length, λ.

Taken together, these experiments highlighted that λ is not only controlled by the brain but also its control is related with others neurophysiological and anatomical features (λ*).

In this framework, Feldman (**2011**) suggested the following rule for muscle activation and force:

Threshold muscle length (λ*):

$$\lambda^* = \lambda - \mu v + \rho + \varepsilon(t) \qquad (1)$$

Where λ* is the dynamic threshold muscle length, composite (net) threshold; λ is it central component; μ is a temporal parameter correlated to the dynamic sensitivity of muscle spindle afferents regulated by γ–motoneurons; v is velocity of change in muscle length, $v > 0$ for muscle stretching and $v < 0$ for muscle shortening; ρ is in the threshold resulting from the intermuscular reflex interaction, i.e. reciprocal inhibition and form cutaneous stimuli; ε(t) is the temporal shift in the threshold resulting from intrinsic properties of motoneurons.

Muscle is active if the actual muscle length (x) exceeds the threshold length, λ*:

$$x - \lambda^* > 0 \quad (1.2)$$

According to rule (1.2), muscle begins to be recruited (activated) if the difference between the current muscle length and dynamic threshold muscle length (λ*) is positive, if not the motoneurons and muscle are silent.

Muscle activation is proportional to:

$$A = [x - \lambda^*]^+ \quad (1.3)$$

The activity (A) of the muscle is related to the difference between the actual and the threshold muscle length, if the difference increases there is an increasing of recruited motoneurons leading to a greater muscle activity.

Motor force (F) is a function (*f*) of:

$$F = f(A, v, t) \quad (1.4)$$

Where v is velocity; t is time.

Muscle action emerges from the tendency to minimize the difference between current muscle length (x) and λ*.

The range of λ regulation, [λ–, λ+], is greater than the biomechanical range of changes in the muscle length, [x–, x+]. In other words, CNS is able in healthy subjects to activate or, conversely, relax muscle at any length within the whole biomechanical range [x–, x+]. To meet these requirements, the threshold must be able to be controlled in a range, [λ–, λ+] that exceeds the biomechanical range. To fully relax a muscle, λ* is shifted beyond the upper biomechanical limit of the range of muscle length. On the contrary, to activate a muscle at its shortest length, the neural control shifts the threshold below the lower biomechanical limit of the joint.

Recently, the range of λ regulation has been explored in adults and children with brain lesions (Jobin and Levin **2000;** Levin et al. **2000;** Musampa et al. **2007;** Mullick et al. **2013**) showing that the impairments in agonist-antagonist muscle activation are related to limitations in the range of regulation of the of the thresholds of muscle activation. In addition, these studies showed that deficits in the control of λ due to CNS damage, resulting in motor deficits including spasticity, weakness as well as impaired inter- joint coordination (reviewed in Levin **2014**). Taken together, these findings support the importance of threshold regulation in the control of movement.

The EP hypothesis, as mentioned earlier, has been extended from the control of one muscle to the control of multi-degree of freedom joint.

The control of a simple joint crossed by two muscles, an agonist and an antagonist, is defined by its own threshold muscle length, λ_{AG} and λ_{ANT}, respectively (**Figure 1.4**, dashed curves). These invariant characteristics describe the overall joint compliant characteristic (JCC) defined by the algebraic sum of the two (**Figure 1.4**, solid line). The control of the joint is achieved according to the combination of λ_{AG} and λ_{ANT} $\{\lambda_{AG} ; \lambda_{ANT}\}$. An equivalent pair of variables can be used to describe the joint behavior, the reciprocal and the co-activation command {r; c} (Feldman **1980**) that reflects the midpoint coordinate between $\{\lambda_{AG} ; \lambda_{ANT}\}$ and the distance between the two $\{\lambda_{AG} ; \lambda_{ANT}\}$, respectively. {r; c} pairs can be defined as:

$$r = (\lambda_{AG} + \lambda_{ANT}) / 2 \quad (1.5)$$

$$c = \lambda_{AG} - \lambda_{ANT} \quad (1.6)$$

Changing the r-command leads to a motion of the joint, this corresponds to a unidirectional shift of λ_{AG} and λ_{ANT}. The c-command describes the shifts of λ_{AG} and λ_{ANT}

in opposite direction, resulting in a change of the apparent stiffness of the joint (**Figure 1.4**)

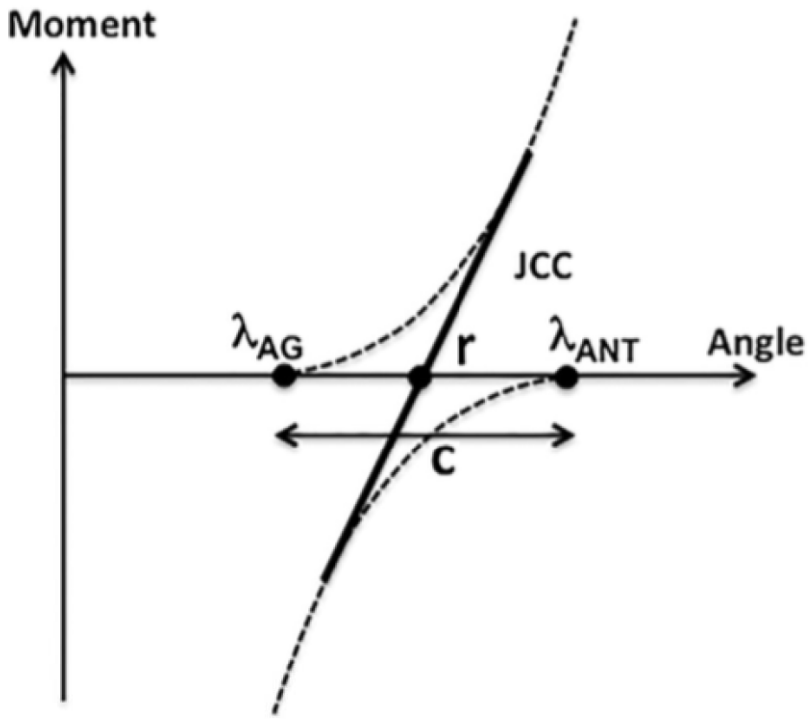

Figure 1.4: Control of a simple joint crossed by two muscles. Joint compliant characteristic (JCC) is defined by the threshold muscle length λ_{AG} and λ_{ANT}, agonist and antagonist muscle, respectively. Dashed curves represent their invariant characteristics. r-command corresponds to the midpoint between λ_{AG} and λ_{ANT}; c-command corresponds to the range between λ_{AG} and λ_{ANT}. From (Latash and Zatsiorsky **2015**)

The idea that CNS controls muscles activation by means of λ regulation (Feldman **1966**, **1986**) has been generalized to the control of the whole body considered as a coherent unit, controlled by a global factor, i.e., the difference between the actual (Q), emerging configuration of the body and its threshold (referent) configuration (R) regulated by the nervous system. In other words, the CNS sets a R of the body at which all the muscles are at the threshold (λ) of activation.

Motor action emerges following the tendency to minimize the difference between the actual position (Q) and the referent body configuration (R) taking into account the anatomical and internal constrains (St-Onge and Feldman **2004;** Feldman **2011**). This minimization process is related to the principle of minimal action in the functioning of the neuromuscular system (Gelfand and Tsetlin **1971**). Within the referent configuration (RC) hypothesis the system tries to achieve a minimum at each level of threshold control. The functioning of the whole system is guided by the tendency to reach activity minima at all levels, in the limits defined by internal and external constraints, form a single motoneuron or muscle level (i.e., threshold muscle length, λ) to the whole body in the environment (referent configuration, RC):

$$A = f\,(AC - RC) \qquad (1.7)$$

Where A is activity (e.g., EMG activity). The movement will proceed until the difference between AC (actual configuration) and RC (referent configuration) becomes minimal, which is achieved when neurons, including motoneurons, also minimize their activity.

The minimization process has been confirmed in several studies that shown the presence of a global minima in the EMG activity of multiple skeletal muscles at certain phases of several complex movements involving multi-degree of freedom joints such as walking, sit-to-stand, gait and drawing-like movements that resemble the Jeté in skilled ballet dancers as well as in hand movements (St-Onge and Feldman **2004;** Lepelley et al. **2006;** Feldman et al. **2011;** reviewed in Feldman **2015**).

1.3 Referent configuration and hierarchical control

Further, the idea of referent configuration has been recently addressed in a multi-level scheme of hierarchical control of motor action organized in a synergic way (see later, 1.1 The Uncontrolled Manifold Hypothesis and Synergies) with low-latency back-coupling loops (Latash et al. **2005;** Martin et al. **2009;** Latash **2010**) . At each level, the CNS defines spatial referent coordinates (RCs) for salient variables, while performance variables (e.g., forces or muscle activations) emerge taking into account the interaction with the environment (see, **Figure 4.1**).

Within this scheme, the task corresponds to the top level (RC_{TASK}), further a chain of few-to-many mappings results in the regulation of λs (lowest level involved) for individual muscles:

$$RC_{TASK} \Rightarrow RC_{JOINTS} \Rightarrow RC_{MUSCLES} \Rightarrow \{r; c\} \Rightarrow \lambda \qquad (1.8)$$

At the joint level, for each axis of rotation, two RC_{JOINTS} are defined, addressed as the reciprocal and the co-activation command {r; c}. Ultimately, at muscles level each {r; c} pair leads to changes in λ of the participating muscles. Within the above-mentioned scheme, each of the few-to-many mappings (i.e., RC_{JOINTS} to λs muscles) is redundant, as the RC_{TASK} dimensionality is smaller than that all the sets of muscles control variable (λs) (Latash **2010**).

Within the prosed definition of living systems (Latash **2016a**, **2016b**), the EP hypothesis has been assumed as a new physical law linking two mechanical variables, muscle length and force, with one modifiable parameter (threshold muscle length, λ). The two mechanical variables are linked following a chain of basic physical laws (Latash **2016b**). At upper level, if we consider a simple joint (**Figure 1.4**) crossed by two

muscles (agonist and antagonist), the parameters, r-command and c-command controlled by the CNS, have been addressed as the two parameters of a physical law salient for the joint level (Latash **2016a**). Further, according to the hypothetical proposed scheme of hierarchical organization of motor elements, the RC_{TASK} represents the controlled parameters of the new physical law emerging at the top level of the hierarchy.

1.4 Motor redundancy and the principle of abundance

The hypothesis of hierarchical control with referent configurations (RC) structured in a few-to-many mappings (Latash **2010**) arises the question how each level is organized to provide stability and coordination during motor actions, i.e., the number of parameters describing motor behavior at higher level, RC_{TASK} , is smaller than the number of parameters defining the same action at lower levels, λs. Indeed, at any level of analysis of motor actions there are more elements than the number of constraints associated with typical tasks (Bernstein **1967**). For example, one can perform a reaching task with the arm involving at least seven major axes of joint rotation, i.e., seven rotational degree-of-freedom, in the 3-dimensional space using a large number (even an infinite number) of solutions to achieve the task successfully, or considering the torque generated at individual joint level there are more than one muscle involved. In other words, the CNS has an infinite number of possibility to perform the same task during everyday movements, similar to solving *n* equations with *m* unknowns, $n < m$ (Latash **2012**).

How the CNS defines a unique action from many possible actions (infinite number) related to the motor task has been addressed as the problem of motor

redundancy (Bernstein **1967**) and it is considered one of the fundamental question in motor control (Turvey **1990**). Bernstein (**1967**) highlighted that the central problem of motor control is "the elimination of degree of freedom", as the ability of the CNS to produce specific movement patterns from an infinite possibility.

Most approaches to the motor redundancy problem have been developed trying to solve how the CNS controls (eliminates) the redundant degrees of freedom leading to a single movement pattern.

One idea is that the CNS limits the set of solutions adding constraints to the neuromotor system. Examples of "elimination of degrees of freedom" may include (1) the size principle of recruitment of motor units (Henneman et al. **1965**), i.e., motor units are recruited according to the size of their alpha-motoneurons, from smallest to largest; (2) the Donder's law, which states that, eye movements are performed with a reduction (constrain) in the number of rotational d from three to two, when the head is stationary. The former example (1) only constraints the possible patterns of motor units recruitment alleviating but not solving the problem of motor redundancy (Latash and Zatsiorsky **2015**). The latter (2) has been demonstrated in some four degrees of freedom arm movements but not observed in movements involving more than four degrees of freedom (Gielen et al. **1997**).

The other approach used to address the motor redundancy problem has been based on optimization principles (reviewed in Prilutsky and Zatsiorsky **2002**). Within this framework, the main idea is based on a function (i.e., a cost function) of variables carried out by individual degrees of freedom and choose a solution that optimizes (minimizes or maximize) the value of the function. According to optimization the

degrees of freedom are reduced by applying a cost function that limits to a unique solution. There are several examples of optimization approaches based on engineer, mechanical and psychological models: minimum time (Enderle and Wolfe **1987**), minimum torque change (Uno et al. **1989**), minimum jerk (Flash and Hogan **1985**), minimum effort (Hasan **1986**), minimum discomfort (Cruse and Bruwer **1987**) and more complex cost functions (Rosenbaum et al. **2001**).

Among the most recent mathematical methods proposed is optimal feedback control (Todorov and Jordan **2002**). Interestingly, this method suggests a flexible behavior to achieve a desired goal without finding a unique for movement production. However, optimal feedback control is based on computations within the CNS.

Recently, the problem of motor redundancy has been reformulated as the principle of motor abundance (Gelfand and Latash **1998;** Latash **2000**, **2012**). According to this principle, the CNS does not compute or select a single solution (i.e., does not attempt to eliminate redundant degrees of freedom), but facilitates families of solutions equally able to perform the task. This approach underlies that the CNS uses all the available degrees of freedoms to accomplish the task and to provide stability of task-specific performance variables within the redundant space of elemental variables.

This principle follows an earlier idea developed by Gelfand and Tsetlin (**1971**) that systems of different complexity are not controlled individually but organized into task specific structural units (principle of non-individualized control). One of the axiom introduced to define proprieties of structural unit was Axiom #3b: "All elements of a structural unit find their own places within a task." This axiom illustrates the principle of abundance, when a redundant set of elements then necessary are involved in

activity of a structural units with regard to each task (Gelfand and Latash **1998;** Latash **2000**).

Arguably, the most famous experiment about motor redundancy (abundance) was performed by Bernstein almost one century ago, in the 1920s. Bernstein recorded the kinematics of the arm of professional blacksmiths hitting a chisel with a hammer, using his novel motion analysis device (kimocyclograph). He discovered that high variability in the individual joint trajectory (i.e., joint angle space) of the arm across repetitive movements was associated with low variability of the hammer trajectory. In other words, the professional blacksmiths performed arm movements in a such way to keep the hammer trajectory invariant using flexible solutions within the motor elements. Joint trajectories showed high intertrial variability, highlighting that not a single solution was reproduced but joints rotation covaried across trails to provide stability of the hammer trajectory.

1.5 The Uncontrolled Manifold Hypothesis and Synergies

The principle of abundance is linked to the notion of task-specific stability initially developed by Schöner (**1995**). According to this idea, a task-specific stability of a particular performance variable can be achieved organizing set of elemental variables within a subspace which the performance variable does not change. This subspace has been addressed as the uncontrolled manifold (UCM)(Scholz and Schoner **1999**) for that performance variable.

For example, during a pointing task, individual joint angles (i.e., elemental variables) co-vary to stabilize the resultant trajectory (i.e. performance variable). Therefore, given a particular value of a task variable (e.g., multi-digit prehension

pointing, reaching), the UCM is the set of all joint configurations that lead to that same value of the performance variable.

The UCM hypothesis is an attractive procedure to test if trial-to-trail variability (i.e., intertrial variance) of elemental variables shows an organization stabilizing a particular performance variable. The UCM allows to quantify the variance of the elemental variables in two components: one that does not affect the performance variable (within the UCM) and one that does (orthogonal to the UCM). For example, consider a simple task of pressing with two fingers to produce a specific total force magnitude (e.g., 10 N), performed several times. Any combination of the finger force that leads to the desired total force magnitude belongs to the UCM, on the other hand any combination of finger force that differ from the task (i.e., the performance is not stabilized) deviates from UCM. Then, an analysis of the variance is performed within the UCM and orthogonal to it.

Recently, according to this framework has been described the concept of synergies (Latash et al. **2007;** reviewed in Latash **2008**).

Synergy has been defined as "a neural organization of a multi-element system that (1) organizes sharing of a task among a set of elemental variables; and (2) ensures co-variation among elemental variables with the purpose to stabilize performance variables" (Latash et al. **2007**). In other word synergies ensure stability of a performance variable while allowing variability of elemental variables (co-variation).

Quantitive analysis of synergies has been developed using the UCM hypothesis reflecting how flexible solutions are used to stabilize a particular performance variable. It is performed comparing the amounts of the total inter-trial variance of elemental

variables per degree of freedom within the UCM (where performance variable is unchanged) with that orthoghonl to the UCM (ORT, where the performance variable changes). Further, an index of synergy (ΔV) can be quantified:

$$\Delta V = \frac{V_{UCM} - V_{ORT}}{V_{TOT}} \quad (1.9)$$

Where V_{UCM} is the variance within the UCM; V_{ORT} is the varince orthogonal to the UCM; V_{TOT} is the total variance. V_{UCM}, V_{ORT} and V_{TOT} are normalized by their respective degrees of freedom. If $V_{UCM} > V_{ORT}$ (i.e., $\Delta V > 0$) a conclusion can be drawn that the performance variable is stabilized in the action.

Several studies have been performed to quantify synergies stabilizing different performance variables within spaces of different sets of elemental variables (reviewed in Latash **2008**). In particular, the structure of the inter-trail variance to estimate the stability has been quantified for multi-digit pressing and prehension tasks, multi-joint reaching tasks, and multi-muscle whole-body tasks (Latash et al. **2007;** Latash and Zatsiorsky **2015**). Moreover, synergies have been explored across populations of neurological patients, allowing to quantify impairments in the neural control of action stability (reviewed in Latash and Huang **2015**).

1.6 Analysis of Synergies

As mentioned earlier, the use of the UCM offers a computational apparatus allowing to study and quantify synergies in different spaces of elemental variables. Several steps are involved in the computation of the UCM: 1) Identify elemental variables; 2) Identify a performance variable (PV); 3) Compute the UCM for the selected PV; 4) Compare variance across trials per degrees of freedom within the

UCM and orthogonal to it.

The first step 1) Identify elemental variables is related to the desired level of analysis. The elemental variables have to be redundant with respect to the task performed, as synergies are based on variance analysis, and elemental variables are expected to present covariation to ensure the stability of the performance. One the other hand, if the elemental variables are not redundant only a single solution exists, and the concept of synergy becomes not applicable. Another important aspect is that elemental variables are assumed to be changed by the neural control independently of each other, i.e., one at a time.

In kinematic studies, individual axes of joint rotation are address as elemental variable. In multi-finger and multi-muscle synergies studies, finger modes and muscles modes have been introduced, respectively, in order to overcome the prerequisite of mutual independence of elemental variable. Within multi-finger studies a finger mode is hypothetical neural command of each specific finger, but each mode leads to force production by all fingers due to enslaving (Zatsiorsky et al. **1998;** Latash et al. **2001**).

A related approach has been applied to multi-muscles synergies studies with the introduction of the notion of muscles modes. Muscle modes have been defined as groups of muscles that show parallel scaling of changes in their levels of activation (Krishnamoorthy et al. **2003a;** Krishnamoorthy et al. **2003b**). Indeed, since the times of Hughlings Jackson (**1889**) which wrote "The brain does not know muscles, it knows only movements, researchers agree that the CNS does not control each muscle independently but rather grouping muscles (i.e., muscles are not activated independently of other muscles). Several computation methods have been developed

to identify muscle modes, such as correlation analysis, principal component analysis (PCA), or non-negative matrix factorization techniques (see Methods). Different methods of matrix factorization resulting in similar findings (Tresch et al. **2006**)

The second step is related to formulate a control hypothesis (Scholz and Schoner **1999**), i.e., if the performance variable is stabilized or not by covariation among the selected elemental variables. Within the framework of synergy, the control hypothesis can be addressed as: "Is there a synergy within a such-and-such space of elemental variables with respect to such-and-such performance variable?" (Latash et al. **2007;** Latash **2008**). Within multi-muscles synergy studies have been shown that centre of pressure trajectory in the anterior-posterior direction is a performance variable stabilized by the covariation of muscles mode. (Krishnamoorthy et al. **2003a;** Danna-Dos-Santos et al. **2007**).

The third step is to compute the UCM for the selected performance variable. At this point relations between small changes in the magnitudes of elemental variables and in the selected performance variable are computed and united into the Jacobian matrix, J. The null-space of J can be used as a linear approximation of the UCM. In kinematic studies the J is a matrix of relations between small changes in joint angles and changes in a performance variable based on the geometrical properties of the system. Within studies of multi-muscle synergies, J matrix has to be defined experimentally (Krishnamoorthy et al. **2003a**) (see Methods).

The last step is analysis of intertrial and interatrial variance. In this phase projections of variance in the space of elemental variables are computed onto the

UCM (V_{UCM}) and orthogonal (V_{ORT}) to it (see Methods). Further, V_{UCM} are V_{ORT} normalized by the number of degrees of freedom in the corresponding sub-spaces. If $V_{UCM} > V_{ORT}$, the hypothesis that the elemental variables covaried to stabilize the performance variable is confirmed. Moreover, the strength of the synergy can be described by ΔV (see equation 1.9), in which postive values correspond to a synergy stabilizing the performance variable, with respect to the elemental variables analyzed.

Within synergy studies a recent phenomenon has been discovered named anticipatory synergy adjustments (ASAs). It was addressed as a mechanism of feedforward control (Olafsdottir et al. **2005**) reflecting an ability of the nervous system to adjust stability properties in preparation for a quick action, leading to an attenuation of the synergy index stabilizing a variable (e.g., change in a force production during accurate force production or change in COP coordinate during whole-body postural tasks) in preparation to a quick change in that variable (see later).

1.7 The feed-forward control of posture: anticipatory synergy adjustment and anticipatory postural adjustment

Maintaining vertical posture by humans is a challenging mechanical task given the relatively high location of the center of mass and relatively small support area. In this study, we focus on feed-forward mechanisms of postural control acting when a standing person is subjected to a predictable, frequently self-initiated, perturbation (e.g., making a fast arm movement or releasing a load).

One of these mechanisms, anticipatory postural adjustments (APAs), has been known for about half a century (Belen'kii et al. **1967;** reviewed in Massion **1992**). APAs

represent changes in the activation levels of postural muscles in preparation to a self-initiated action associated with perturbation of the vertical posture. Such changes may be seen starting about 100 ms prior to the action initiation. Their function has been assumed to generate net forces and moments counteracting those expected from the perturbation (Cordo and Nashner **1982;** Bouisset and Zattara **1987;** Ramos and Stark **1990**). Consistent with this hypothesis, APAs change their patterns when the direction of perturbation changes (Aruin and Latash **1995**).

The second feed-forward mechanism, anticipatory synergy adjustments (ASA), has been described relatively recently (Olafsdottir et al. **2005;** Shim et al. **2005**). During whole-body tasks performed by standing persons, ASAs represent changes in an index of a multi-muscle synergy stabilizing the coordinate of the center of pressure (COP). Such changes may be seen in young, healthy persons about 200-300 ms prior to the action initiation (Klous et al. **2011;** Krishnan et al. **2011;** Krishnan et al. **2012**), significantly earlier than APAs.

The purpose of ASAs has been assumed to facilitate a change in a salient performance variable (such as COP coordinate) and avoid fighting one's own synergies stabilizing that variable. Note that similar ASAs are expected independently of the direction of a perturbation, e.g., forward or backwards, since a quick reactive COP shift in the anterior-posterior direction is needed to stabilize posture across conditions.

1.8 Aims and Hypothesis

The two mechanisms, APAs and ASAs, may be expected to show different degrees of specificity with changes in the direction of a self-triggered perturbation. To explore this prediction, we compared APAs and ASAs in standing subjects who

performed similar actions that could lead to postural perturbations in two opposite directions. In some series, the subjects knew the direction of the perturbation in advance, while in other series, this direction varied randomly across trials.

To study these feed-forward control mechanism, we quantified APAs and ASAs in subjects performing a load-release task, which is typically associated with pronounced APAs (Aruin and Latash **1995**).

ASAs were analyzed using the framework of the uncontrolled manifold (UCM) hypothesis (Scholz and Schoner **1999;** Latash et al. **2007;** reviewed in Latash **2008**). As explained above, this method quantifies inter-trial variance within a set of elemental variables (M-modes, muscle groups with parallel changes in activation levels, (Krishnamoorthy et al. **2003a**)) in directions that lead to no changes in a salient performance variable (UCM for that variable) and in directions orthogonal to the UCM (ORT) leading to changes in the salient variable. Further, an index of synergy is computed reflecting the difference between the variance components, $\Delta V = (V_{UCM} - V_{ORT})/V_{TOT}$ normalized by total variance (V_{TOT}). Multi-M-mode synergies were quantified for COP coordinate in the anterior-posterior direction (COP_{AP}) as the salient performance variable.

1.8.1 Hypothesis-1

Our Hypothesis-1 was that ASAs would not show changes in their characteristics across series with known and unknown directions of perturbation (based on a study of multi-finger synergies (Zhou et al. **2013**), see Discussion).

1.8.2 Hypothesis-2A and 2B

Our second hypothesis was that APAs would be sensitive to information on direction of perturbation. For trials with perturbations with randomly changing direction, we expected two changes in APAs as compared to conditions with known perturbation direction. First, APAs could reduce and even disappear (Hypothesis-2A) since a strong APA in a "wrong direction" could contribute to postural destabilization. Second, APAs could change their patterns. While young, healthy persons typically show reciprocal patterns of activation in agonist-antagonist postural muscle pairs during APAs (Bouisset and Zattara **1987;** Aruin and Latash **1995**), persons with impaired postural control tend to show parallel changes in activation of agonist-antagonist muscles (co-contraction patterns; (Woollacott et al. **1988;** Schmitz et al. **2002;** Chen et al. **2015**). Co-contracting agonist-antagonist muscles produces little net force/moment but increases the apparent stiffness of the joint (Latash and Zatsiorsky **1993**), which reduces kinematic consequences of any force perturbation. So, we also expected a change from a typical reciprocal APA pattern in conditions with known direction of perturbation to a co-contraction pattern in conditions when the direction of perturbation was unpredictable (Hypothesis-2B).

2 METHODS

2.1 Subjects

Eleven healthy subjects (6 males and 5 females, age 28.5 ± 4.7 years, mass 67.95 ± 11.66 kg, and height 1.67 ± 0.10 m; mean ± SD) without any known musculoskeletal or neurological impairments took part in the experiment.

All participants were right-handed based on their own disclosure about preferential hand use during daily activities such as writing and eating. All subjects gave their informed consent according to the procedures approved by the Office for the Research Protections of the Pennsylvania State University.

2.2 Apparatus

A force platform (AMTI, OR-6) was used to record the vertical, anterior–posterior and medio-lateral components of the ground reaction force (F_Z, F_X and F_Y, respectively) as well as the moments of force around the frontal and sagittal axes (M_Y and M_X, respectively). Surface muscle activation (EMG) signals were recorded using a 16-channel Trigno Wireless System (Delsys Inc., MA, USA). Active electrodes with built-in amplifiers (rectangular shape, 37 mm × 26 mm × 15 mm) were attached with adhesive tape to the skin over the bellies of the following thirteen muscles on the right side of the body: tibialis anterior (TA), soleus (SOL), gastrocnemius lateralis (GL), gastrocnemius medialis (GM), biceps femoris (BF), semitendinosus (ST), rectus femoris (RF), vastus lateralis (VL), vastus medialis (VM), tensor fasciae latae (TFL), lumbar erector spinae (ESL), thoracic erector spinae (EST), and rectus abdominis (RA). The electrode placement was confirmed by asking the subjects to perform a set of

isometric contractions and related free movements while observing the resulting EMG patterns (Kendall et al. 2005). EMG signals were pre-amplified and band-pass filtered (20 – 450 Hz) before being transmitted to the base station connected to the data collection computer (Dell, Core i7 2.93Ghz). A customized LabVIEW-based software (LabVIEW 2013 - National Instruments, Austin, TX, USA) was used to acquire and record EMG and force platform signals sampled at 1 kHz with 16-bit resolution data acquisition board (PCI- 6225, 250 kS/s, 80 Analog Inputs Multifunction DAQ, National Instruments).

2.3 Procedures

In the initial position, subjects were standing barefoot on the force platform with their feet in parallel at hip width (the insides of the feet 15 cm apart). This foot position was marked on the top of the platform to make this initial position consistent across all trials and conditions. A 21" monitor positioned 1.5 m in front of the participants at the eye level was used for visual feedback. Each experimental session consisted of four tasks: 1) quiet standing, 2) control trials, 3) voluntary body sway task, and 4) load-release task.

The quiet standing and control trials were performed to normalize EMG signals (see the next section). In the quiet standing task, subjects were instructed to stand quietly on the force platform with arms by sides and to look at a fixed point on the wall in front of the subject, while trying to prevent any body movements for 30 s.

In the control trials, subjects were asked to hold a handle bar by grasping the two circular panels at each side of the bar with both hands with the shoulders flexed at 90° and elbows fully extended (**Figure 2.1A**). The bar was connected to a pulley system

that allowed using the 5 kg load to generate either a downward force (the load was suspended from the middle of the bar; control trial #1), or an upward force (the load was acting through the pulley system behind the subject's body; control trial #2). This posture was held for at least 10 s with a one-minute rest period between the two conditions. During both control trials, the subjects were asked to stand still, without forward or backward movement (controlled by the experimenter).

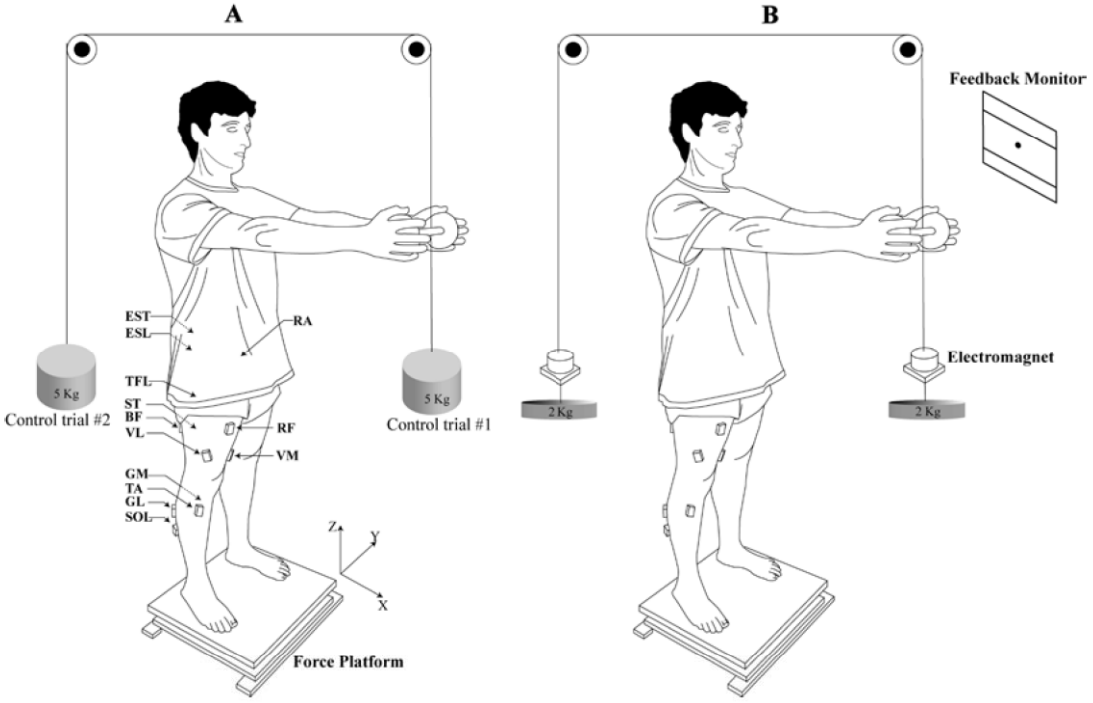

Figure 2.1: (A) Schematic illustration of the control trials. In the control trial #1 a load (5 kg) was suspended from the middle of the bar in front of the subject. In the control trial #2 the load was connected through the pulley system behind the subject's body. (B) Schematic representation of the load release trials. Subjects triggered perturbation by releasing a load (2 Kgs) attached to the electromagnets through the pulley system. Location of the EMG electrodes is shown (TA - tibialis anterior, SOL - soleus, GM - gastrocnemius medialis, GL - gastrocnemius lateralis, BF - biceps femoris, ST - semitendinosus, RF - rectus femoris, VL - vastus lateralis, VM - vastus medialis, TFL - tensor fasciae latae, RA - rectus abdominis, EST - thoracic erector spinae, ESL - lumbar erector spinae)

In the voluntary body sway task (**Figure 2.2**), subjects were instructed to occupy an initial position with the arms crossed over the chest and fingertips placed on the shoulders, and to perform continuous voluntary full-body sways about the ankle joints in the anterior–posterior (AP) direction (Danna-Dos-Santos et al. **2007;** Klous et al. **2011**). The frequency of the sway was set at 0.5 Hz, paced by an auditory metronome. A continuous visual feedback was provided on the subjects' center of pressure (COP) displacement, in the anterior-posterior (COP_{AP}), and in the medial-lateral direction (COP_{ML}). These were computed on-line using the following equations (Winter et al. **1996**):

$$COP_{AP} = -\frac{M_y+(F_x \cdot d_z)}{F_z} \quad (2.1)$$

$$COP_{ML} = \frac{M_x+(F_y \cdot d_z)}{F_z} \quad (2.2)$$

In these equations, d_z represents the distance from the surface to the platform origin (0.043 m). The amplitude of COP_{AP} shift displayed on the monitor was set at ± 3 cm forward and backward, symmetrical with respect to the initial COP_{AP} coordinate. The target amplitude was presented on the screen as a pair of target lines while the instantaneous COP coordinate was shown as a 5-mm white circle. A period of practice was given to each subject prior to data acquisition. The task was performed twice; the duration of each trial was 30 s with a 30-s rest period between trials. Subjects were asked to do their best to minimize COP deviations in the medio-lateral direction and to keep full contact of both heels and toes with the platform surface during the sway (observed by the experimenter).

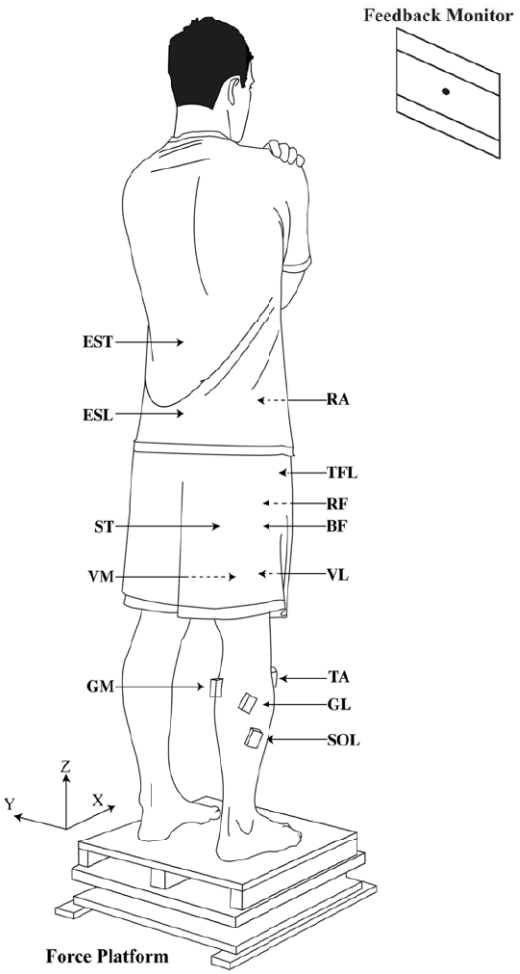

Figure 2.2: Schematic illustration of the control body sway task. The arms were crossed on the chest with the fingertips placed on the shoulders. Subjects were asked to sway for 30 s while keeping the feet on the force plate, within an amplitude of COP_{AP} ± 3 forward and backward. The frequency of the sway was set at 0.5 Hz, paced by a metronome. Location of the EMG electrodes is shown (TA - tibialis anterior, SOL - soleus, GM - gastrocnemius medialis, GL - gastrocnemius lateralis, BF - biceps femoris, ST - semitendinosus, RF - rectus femoris, VL - vastus lateralis, VM - vastus medialis, TFL - tensor fasciae latae, RA - rectus abdominis, EST - thoracic erector spinae, ESL - lumbar erector spinae)

In the load-release tasks, subjects occupied the initial body position while holding the handle bar, in the same position as described above for the control trials. Then, they were requested to lean forward, such that their COP_{AP} matched a target line 3 cm from the initial COP_{AP} coordinate. Leaning forward was used to ensure a non-zero level of background muscle activation, which was necessary to perform further analysis of multi-muscle synergies (as in earlier studies (Klous et al. **2011;** Falaki et al. **2016**). While leaning may lead to changes in APAs, these changes are relatively modest (Aruin et al. **1998;** Aruin **2003**). The initial posture was consistent across conditions with predictable and unpredictable directions of unloading (see later).

Two loads of 2 kg each were attached to the pulley system in such a way that one load was in front of the subject and the other load was behind the subject's body (**Figure 2.1B**); as a result, there was no net vertical force acting on the handle. Each load was attached with a cylindrical electromagnet. On the right side of the handle bar, there was a switch that could turn off one of the two electromagnets releasing the corresponding load and leading to a postural perturbation. After reaching the initial steady state, subjects were asked to push the trigger with the right thumb to initiate the load release; this was done in a self-paced manner at any time within a 10-s time window.

The experimenter controlled which of the two electromagnets would be turned off by the switch. Two perturbation directions were studied: Backward (the released load was in front of the subject) and Forward (the released load was behind the body of the subject), under two different conditions where the perturbation direction was either known (Kn) or unknown (Un) to the subject in advance. We will refer to the

conditions as BKn (backward perturbation, known direction), FKn (forward perturbation, known direction), BUn (backward perturbation, unknown direction), and FUn (forward perturbation, unknown direction). There were 24 trials within each experimental series. The direction of perturbation was kept the same and known to the subject in advance within the series BKn and FKn. The order of these two series was randomized across subjects. Two more series included perturbations with directions presented in an unpredictable, balanced order. Over these two series, 24 trials were under the BUn condition and 24 trials – under the FUn condition. In these series, the experimenter asked the subjects not to guess/predict the direction of the load release. In summary, participants always knew in advance the exact timing of the "perturbation" as it was self-triggered, while the direction could be either predictable or unpredictable. The intervals between the 15-s trials were 8-10 s (2-3 trials per minute) with 3-min rest period between conditions; the unpredictable conditions were always presented after the predictable conditions to avoid possible effects of performing the relatively unusual unpredictable conditions on the more familiar predictable conditions.

Prior to data collection, a period of familiarization with the load-releasing task, with 12 trials for each of perturbation directions, was given to each subject. Additional rest periods were provided if requested, none of the subjects reported fatigue. The whole experimental session lasted for about 90 min.

2.4 Data processing

The data were processed and analyzed off-line using a customized Matlab 2015b (MathWorks, Natick, MA) software package. Signals from the force platform (F_Z, F_X, and M_Y) were filtered with the 5 Hz low-pass, 2nd order, zero-lag Butterworth filter before calculating the COP_{AP} and COP_{ML} using equations (2.1) and (2.3).

For each 30-s trial of the body sway task, the data in the interval {3; 28 s} were accepted to avoid edge effects. A cycle was defined as the time between two successive anterior-most COP_{AP} coordinates. On average, each subject performed 12 full cycles within this period.

The onset of the load-release task (t_0) was calculated by a computer algorithm as the point in time when the magnitude of the first time derivative of F_Z exceeded 5% of its peak absolute magnitude in that particular trial. These values were confirmed by visual inspection.

For the load-release task, trials with the following errors were excluded from further analysis: body position was not kept steady prior to t_0 (i.e. COP_{AP} trajectory exceeded ± 2 standard deviations within the time interval {t_0-300 ms; t_0} from the average value of that particular series) and trials with corrupted EMG signals (likely due to electrode-skin detachment). The number of rejected trials per series was 5±1.

Raw EMG signals were full-wave rectified and low-pass filtered by means of a moving average 100-ms window. To account for the electro-mechanical delay (Corcos et al. **1992**), EMG data were shifted 50 ms backward with respect to the force platform data for computations involving both EMG and mechanical signals. In order to compare EMG data across subjects, the processed signals were corrected for

background activity and normalized using the method described in previous studies (Krishnamoorthy et al. **2003a;** Danna-Dos-Santos et al. **2007;** Klous et al. **2010**):

$$EMG_{norm} = \frac{EMG - EMG_{qs}}{EMG_{ref}} \quad (2.3)$$

EMG_{qs} is the average filtered EMG during the quiet stance trial computed within the time interval {13 s; 17 s} and EMG_{ref} is the average filtered EMG in the middle of control trials. For dorsal muscles (SOL, GL, GM, BF, ST, ESL, and EST), EMG_{ref} was calculated from the control trial#1 in which the load was held in front of the subject and for the ventral muscles (TA, VM, VL, RF, RA, and TFL) when the load was acting behind the subject (control trial#2).

2.4.1 Defining muscle modes

The objective of this phase was to identify groups of muscles (muscle modes or M-modes, eigenvectors in the muscle activation space) that showed parallel scaling of changes in their levels of activation. Such muscle groups play the role of elemental variables for the analysis of synergies (see later and (Krishnamoorthy et al. **2003a;** Krishnamoorthy et al. **2003b**). This step reduced the 13-dimensional muscle activation space into a 4-dimensional M-modes space. For this purpose, EMG_{norm} signals from the two voluntary body sway tasks were integrated over 50-ms time windows ($IEMG_{norm}$). For each subject, the $IEMG_{norm}$ data from the two trials were concatenated to create a matrix with thirteen columns representing 13-muscles and the number of rows corresponding to the number of samples across the sway cycles analyzed. Principal component analysis (PCA) with Varimax rotation and factor extraction was applied to the correlation matrix of $IEMG_{norm}$ data (Krishnamoorthy et al. **2003a;** Danna-Dos-Santos et al. **2007**).

For each subject, the first four principal components (PCs) were selected based on the following criteria: The Kaiser criterion and an inflection point in the scree plot after the fourth eigenvalue confirmed by visual inspection, and each PC had to contain at least one muscle with a significantly high loading (with the absolute magnitude over 0.5; (Hair et al. **1995**)).

This procedure produced an orthogonal set of eigenvectors in the muscle activation space, M-modes which were used as the elemental variables for further analysis of M-mode synergies (see section 'Analysis of variance within the UCM hypothesis').

The M-mode magnitudes were computed for each subject for the voluntary body sway task by multiplying the factors (eigenvectors, loadings of the individual M-modes) by the $IEMG_{norm}$ matrix:

$$M_{sway-task} = [eigenvectors] \times [IEMG_{norm}] \quad (2.4)$$

In our study, we applied the same set of M-modes, extracted from the body sway task, to the load-release task, since similar patterns of the synergy indices and M-mode compositions were found in previous studies (Klous et al. **2011;** Krishnan et al. **2011;** Krishnan et al. **2012**).

In line with previous literature on the muscle M-modes composition (Krishnamoorthy et al. **2003a; 2003b;** Danna-Dos-Santos et al. **2007;** Krishnan et al. **2011**), we classified M-modes into "ventral M-modes" (with significantly loaded ventral muscles), "dorsal M-modes" (with significantly loaded dorsal muscles), and "mixed M-modes" (which commonly had TFL and RA significantly loaded).

Within each trial of the load-release task, M-mode magnitudes were calculated by multiplying the EMG_{norm} matrix (formed with 13-columns representing 13-muscles and number of rows corresponding to the number of sample analyzed) within the time window {1000 ms prior to t_0; 300 ms after t_0} by the eigenvectors:

$$M_{load\ release-\ task} = [eigenvectors] \times [EMG_{norm}] \quad (2.5)$$

2.4.2 APA structure time

The time of APA initiation, t_{APA}, was determined for each subject and each condition of the load-release task. The average value and standard deviation (SD) over the steady-state phase {(t_0 – 900) ms ; (t_0 – 300) ms} were calculated for the ventral and dorsal M-modes. Further, t_{APA} was defined as the time when the mode magnitude differed from the average baseline value by ±2 SD. The earliest in time value, across the ventral and dorsal M-modes, was selected as t_{APA}, confirmed visually at optimal resolution.

The EMG changes during APAs were computed for each of the four conditions, for each subject and each muscle separately, by subtracting integrals of the baseline activity, estimated within the time interval {(t_0 – 900) ms; (t_0 – 300) ms} and normalized to time interval of 150 ms, from integrals calculated within {–100 ms +50 ms} with respect to t_0:

$$\int APAdt = \int_{-100}^{+50} EMGdt - \left(\int_{-900}^{-300} EMGdt \right) /4 \quad (2.6)$$

Further, for brevity, we omit the “dt” in expressions including time integrals. For comparison across subjects, ∫APA indices for each muscle were normalized by the

maximal magnitude of this integral across the experimental conditions. Note that after this normalization all the ∫APA values were within the range from +1 to −1 (Slijper and Latash **2000**, **2004**).

To quantify indices of co-activation and reciprocal activation within agonist–antagonist muscle groups at the level of M-modes, integrals of ventral and dorsal M-mode activities were calculated and analyzed (Slijper and Latash **2000**, **2004;** Chen et al. **2015**). We used the same expression as shown in Eq. (2.6) to estimate the changes in M-mode magnitudes.

Subsequently, co-contraction (*C-index*) and reciprocal (*R-index*) indices were computed (Slijper and Latash **2000**, **2004**) within the framework of the equilibrium-point hypothesis (reviewed in Feldman **1986;** Feldman **2015**). Since the baseline activity of the dorsal muscles was greater than that of the ventral ones (due to the initial leaning forward posture):

$R = (\int APA_{ventral\ M-modes} - \int APA_{dorsal\ M-modes})$ and

$C = 0$ if $\int APA_{ventral\ M-modes}$ and $\int APA_{dorsal\ M-modes}$ had different signs;

$C = \min\{|\int APA_{ventral\ M-modes}|\ ;\ |\int APA_{dorsal\ M-modes}|\}$ if $\int APA_{ventral\ M-modes}$ and $\int APA_{dorsal\ M-modes}$ had the same signs.

For comparison across subjects, both *R* and *C* were normalized by the absolute highest values for each series and each subject separately.

2.4.3 Defining the Jacobian matrix

The objective of this step was to define the Jacobian (**J**) matrix that links small changes in M-modes (ΔM) to COP_{AP} displacements (ΔCOP_{AP}), assuming linear relations between these variables (Krishnamoorthy et al. **2003b;** Danna-Dos-Santos et al. **2007**)

ΔM and ΔCOP_{AP} data were computed from $IEMG_{norm}$ and integrated COP_{AP} (within 50-ms time windows) data from the body sway task. Both ΔM and ΔCOP_{AP}, were filtered with a 5 Hz, low-pass, 4th order, zero-lag Butterworth filter (Falaki et al. **2014, 2016**).

Multiple regression analysis was performed for each subject separately:

$$\Delta COP_{AP} = k_1\Delta M_1 + k_2\Delta M_2 + k_3\Delta M_3 + k_4\Delta M_4 \quad (2.7)$$

The resulting set of coefficients from the regression were arranged in a matrix that is the **J** matrix: $\mathbf{J} = [k_1\ k_2\ k_3\ k_4]^T$, where T is the sign of transpose. Hence, this step resulted in one **J** matrix for each subject.

2.4.4 Computation of the synergy index

We used the framework of the UCM hypothesis (Scholz and Schoner **1999;** Latash et al. **2007**) assuming that the central nervous system manipulates a set of elemental variables (M-mode magnitudes) to stabilize a salient performance variable (COP_{AP} coordinate). Specifically, the inter-trial variance in the M-mode space was divided into two components, within the UCM, approximated as the null-space of **J**, where the COP_{AP} coordinate did not change (V_{UCM}) and within the orthogonal complement to the UCM (V_{ORT}). V_{UCM} and V_{ORT} were computed within the four-dimensional M-mode space for each subject separately. The UCM was three-dimensional and the ORT subspace was one-dimensional. Comparing V_{UCM} and V_{ORT}, normalized by the dimensionality of their respective sub-spaces, produces an index of multi-M-mode synergy (ΔV) (Krishnamoorthy et al. **2003b;** Danna-Dos-Santos et al. **2007**) with a fixed value of the COP_{AP} coordinate.

For all the subjects, the residual mean-free values of M-modes ($\mathbf{M_{demeaned}}$) were calculated across all trials within each of the four conditions of the load-release task:

$$M_{demeaned} = \Delta M - \bar{\bar{M}} \quad (2.8)$$

where $\bar{\bar{M}}$ is the mean change in M-modes magnitudes across all trials, **ΔM** is the change in the magnitude of the M-modes for each trial within the time interval {1000 ms prior to t_0; 300 ms after t_0}.

The UCM subspace was approximated as the null-space of the corresponding **J**, i.e., a set of all vector solutions **x** of a system that satisfies the equation **Jx** = 0, which is spanned by basis vectors ε_i. The demeaned vector of M-modes ($M_{demeaned}$) was projected onto the null-space of **J** (UCM) and onto ORT:

$$f_{UCM} = \sum_{i=1}^{n-d}(\varepsilon_i^T \cdot M_{demeaned})^T \cdot \varepsilon_i^T \quad (2.9)$$

$$f_{ORT} = M_{demeaned} - (f_{UCM})^T \quad (2.10)$$

where f_{UCM} and f_{ORT} are projections of $M_{demeaned}$ onto the UCM and ORT, respectively. For each subject and condition, V_{UCM}, V_{ORT}, and the total variance (V_{TOT}), normalized by their respective degrees of freedom, were calculated as follows:

$$V_{UCM} = \sigma_{UCM}^2 = \frac{1}{(n-d)(N_{trials})}\sum_{i=1}^{N}|f_{UCM}|^2 \quad (2.11)$$

$$V_{ORT} = \sigma_{ORT}^2 = \frac{1}{(d)(N_{trials})}\sum_{i=1}^{N}|f_{ORT}|^2 \quad (2.12)$$

$$V_{TOT} = \sigma_{TOT}^2 = \frac{1}{(n)(N_{trials})}\sum_{i=1}^{N}|M_{demeaned}|^2 \quad (2.13)$$

N_{trials} is the total number of trials in each series.

To quantify the relative amount of inter-trial variance compatible with stabilization of COP_{AP}, the index of synergy (ΔV) was computed as:

$$\Delta V = \frac{V_{UCM} - V_{ORT}}{V_{TOT}} \quad (2.14)$$

Since V_{UCM}, V_{ORT} and V_{TOT} were computed per degree of freedom, ΔV ranged between 1.33 (all variance is within the UCM) and -4 (all variance is within the ORT).

For further statistical analysis, ΔV values were log-transformed using modified Fisher's z-transform (Solnik et al. **2013**):

$$\Delta V_Z = \frac{1}{2} \cdot log\left(\frac{|\Delta V_{lower}| + \Delta V}{\Delta V_{upper} - \Delta V}\right) - \frac{1}{2} \cdot log\left(\frac{|\Delta V_{lower}|}{\Delta V_{upper}}\right) \quad (2.15)$$

The changes in the variance indices and the synergy index (ΔV_{UCM}, ΔV_{ORT}, and $\Delta\Delta V_Z$), were quantified as the difference between the mean magnitudes of V_{UCM}, V_{ORT}, and ΔV_Z over the steady-state {($t_0 - 900$) ms ; ($t_0 - 400$) ms} and their respective means about the load release time ($t_0 \pm 25$ ms).

Anticipatory synergy adjustments (ASA) were identified as a drop in the ΔV_Z time profile prior to t_0. The time of ASA initiation (t_{ASA}) was identified as the instant in time when ΔV_Z exceeded 1 SD from the average value over the steady-state phase and stayed below the average value until t_0. The t_{ASA} values were also visually confirmed by an experienced researcher.

2.5 Statistics

Data are presented in the text and figures as means and standard errors (SE). Two-way ANOVA with repeated measures was performed with factors *Direction* (backward vs. forward) and *Condition* (known vs. unknown).

In particular, we explored how the main outcome variables such as ΔV_{UCM}, ΔV_{ORT}, $\Delta\Delta V_Z$, t_{ASA} (Hypothesis-1) and t_{APA} (Hypothesis-2A), R-indices and C- indices (Hypothesis-2B) were affected by these factors. Pairwise contrasts with Bonferroni corrections were used to explore significant effects. In all the repeated measures ANOVA, whenever the Mauchly's test of sphericity was not satisfied, the Greenhouse – Geisser correction was made. We per- formed a two-way MANOVA on *∫*APA values to

test the effects of Direction and Condition on changes in activation of individual muscles during APAs.

The level of significance was set at $p < 0.05$. All statistical analyses were performed with SPSS 21.0 (IBM Corp., Armonk, NY, USA).

3 RESULTS

3.1 Identification of muscle modes and Jacobian

During the cyclical sway task, the subjects showed consistent patterns of muscle activation at the sway frequency. Typically, ventral muscles crossing different joints showed similar time patterns and proportional activation changes; the same was true for the dorsal muscles. These patterns were reflected in consistent muscle groups (M-modes, see Methods) identified in our study using the PCA with rotation and factor extraction applied to integrated indices of muscle activation. On average, the four rotated PCs (M-modes) accounted for 79.2 ± 1.6% (ranging from 78.2 to 85.9%) of the total variance.

A typical set of M-modes is presented in Table 3.1 with the significant loadings shown in bold. Loadings at individual muscles for the first two PCs were similar across subjects.

Indeed, one of the first two PCs showed high loading values for the dorsal muscles, while the other PC showed high loading values for the ventral muscles. The third and fourth M-modes were more variable across subjects and typically had only one or two muscles significantly loaded (typically, RA or TFL). We saw six cases of significant loadings of the same sign within an agonist-antagonist pair (co-contraction patterns) out of 44 M-modes across all subjects.

Muscle	M1-mode	M2-mode	M3-mode	M4-mode
TA	-0.268	**0.875**	0.054	0.180
SOL	**0.914**	-0.106	-0.029	0.017
GM	**0.921**	-0.177	-0.021	-0.067
GL	**0.918**	-0.113	-0.044	0.024
BF	**0.838**	-0.147	0.068	-0.100
ST	**0.804**	-0.400	-0.020	-0.250
VL	-0.275	**0.900**	0.031	0.118
RF	-0.134	**0.811**	0.101	0.201
VM	-0.119	**0.904**	-0.005	0.029
TFL	-0.236	0.357	0.076	**0.874**
RA	0.016	0.100	**0.990**	0.056
EST	**0.864**	-0.175	0.038	-0.237
ESL	**0.852**	-0.297	0.004	-0.209

Table 3.1: The muscle loading factors for the M-modes. Loading factors for the first four PCs after Varimax rotation and factor extraction for a typical subject are shown. Significant loadings (greater than 0.5) are shown in bold. TA - tibialis anterior, SOL - soleus, GM - gastrocnemius medialis, GL - gastrocnemius lateralis, BF - biceps femoris, ST - semitendinosus, RF - rectus femoris, VL - vastus lateralis, VM - vastus medialis, TFL - tensor fasciae latae, RA - rectus abdominis, EST - thoracic erector spinae, ESL - lumbar erector spinae

Linear regression analysis confirmed a significant linear relation between changes in the magnitudes of the M-modes and COP_{AP} shifts. All four M-modes were significant predictors of COP_{AP} shifts in all subjects ($p < 0.001$). On average, the linear regression accounted for 69 ± 2% of the total variance in COP_{AP}.

3.2 Anticipatory postural adjustments (APAs)

During the load-release trials, the subjects were instructed to lean forward before initiating the self-triggered perturbation. As a result, nonzero EMG levels (and M-modes) could be observed, particularly in the dorsal muscles, during steady-state standing. There were consistent changes in the muscle activation levels prior to the self-triggered unloading. **Figure 3.1** shows the typical EMG time profiles for a subset of muscles in a representative subject, averaged across repeated trials with the self-triggered perturbation acting backwards (BKn) and forward (FKn) when the subject knew in advance the perturbation direction. EMG patterns under the conditions with unknown direction of perturbation (FUn and BUn) are shown in **Figure 3.2**. Note the consistent EMG changes prior to the time of action initiation (t_0) shown in **Figure 3.1** with arrows. Under the Kn condition, these changes typically included reciprocal changes in the activation levels within agonist-antagonist pairs: A drop in the activation level of dorsal muscles (sometimes accompanied by an EMG burst in ventral muscles) under the BKn condition and an increase in the activation level of dorsal muscles under the FKn condition.

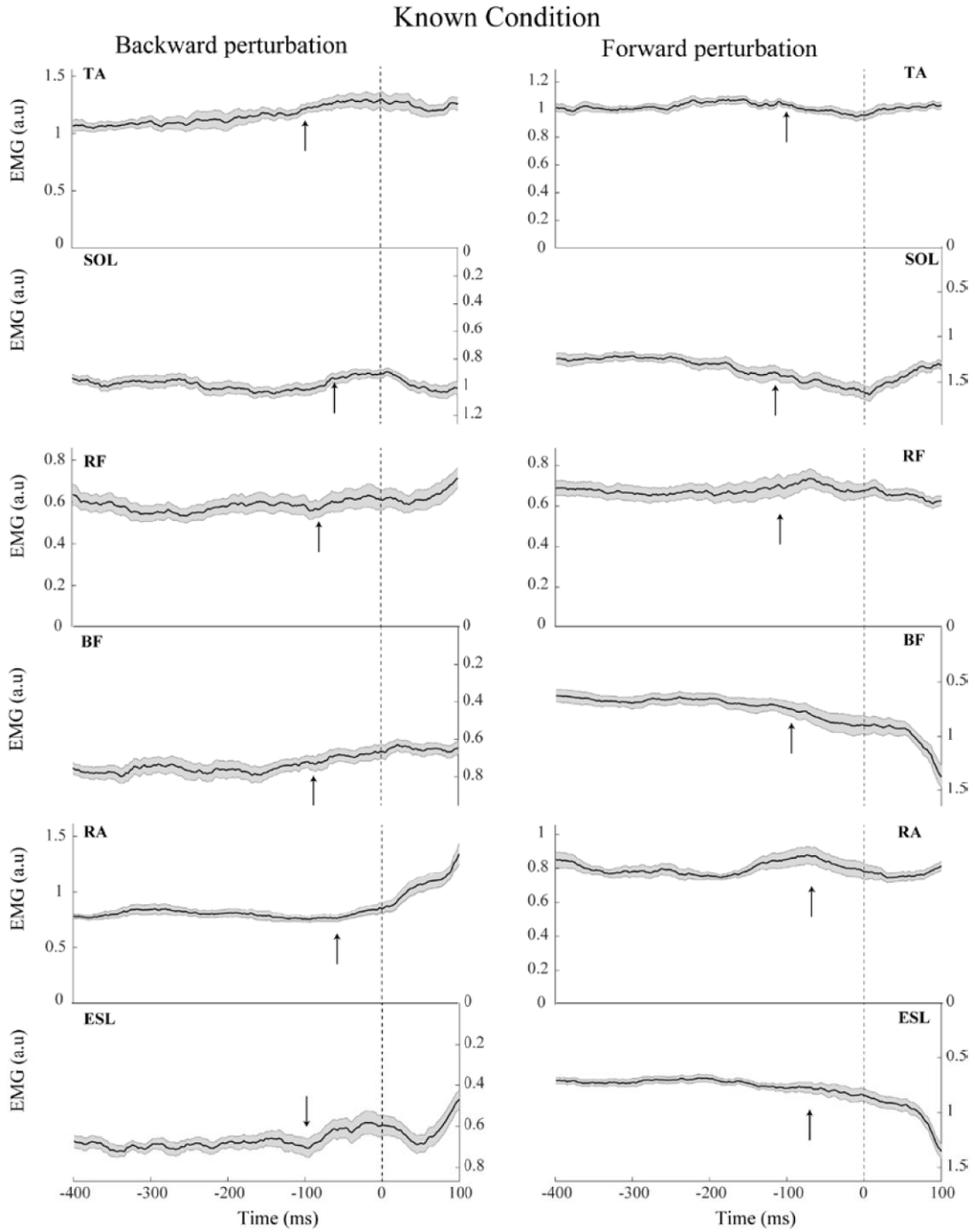

Figure 3.1: EMG time series averaged across trials by a typical subject for the backward (left panels) and forward perturbations (right panels) under the known direction of perturbation. The data for a subset of muscles are presented: tibialis anterior (TA), soleus (SOL), rectus femoris (RF), biceps femoris (BF), rectus abdominis (RA) and lumbar erector spinae (ESL) with standard error shades. The vertical dashed lines show the perturbation time (t0=0). Arrows show the onset of APAs (tAPA). Note the reciprocal activations of muscles before the perturbation onset. EMG activity is in normalized units. EMG signals for SOL, BF, and ESL are inverted for better visualization

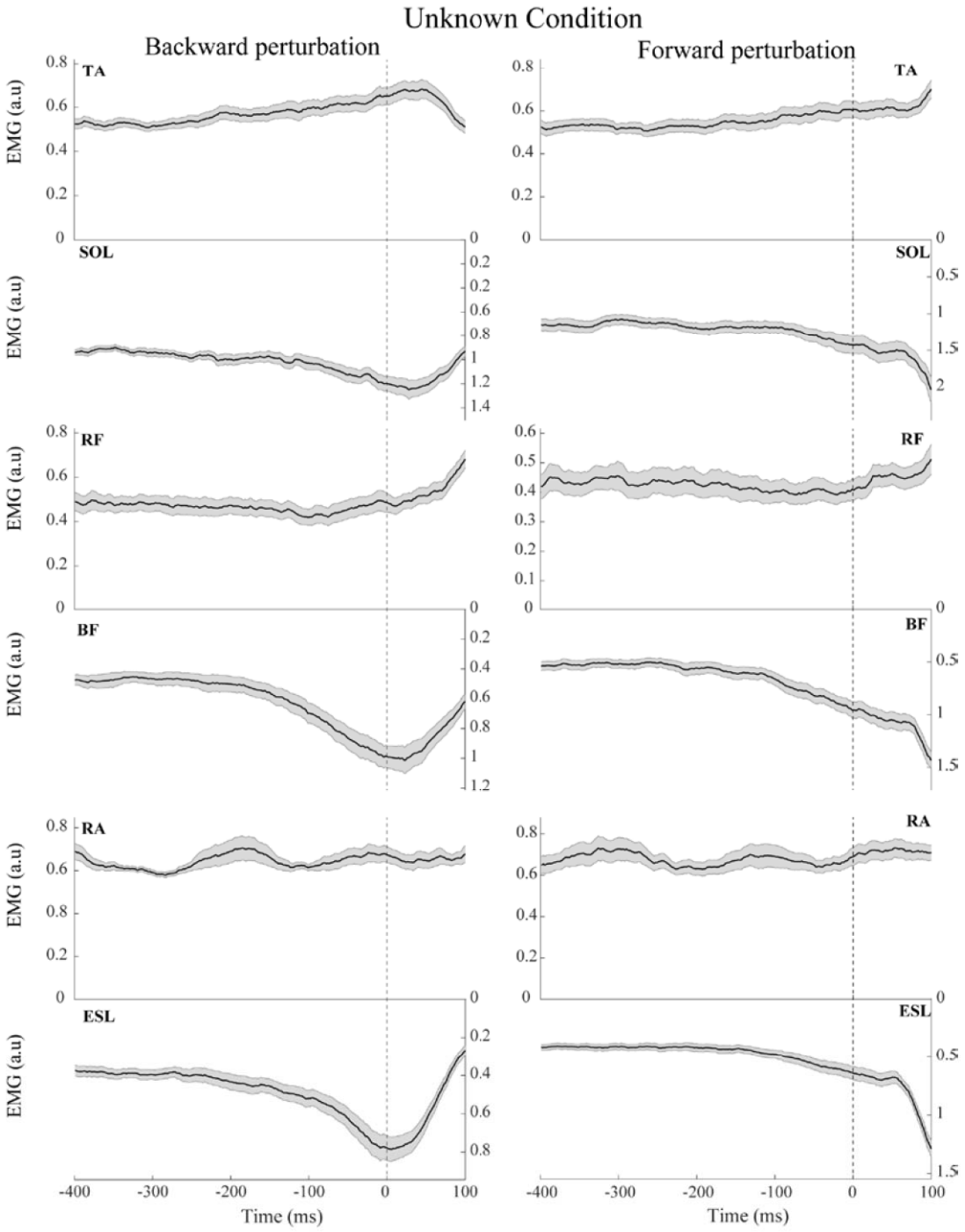

Figure 3.2: EMG time series averaged across trials by a typical subject for the backward (left panels) and forward perturbations (right panels) under the unknown direction of perturbation. The data for a subset of muscles are presented. For abbreviations see Figure 3.1. Note the unidirectional changes in muscle activation levels before the perturbation onset. EMG activity is in normalized units. EMG signals for SOL, BF, and ESL are inverted for better visualization

When the perturbation direction was unknown to the subject, two typical changes were observed. First, t_{APA} shifted toward the action initiation time. Averaged across subjects, t_{APA} magnitude was 117.14 ±17.52 ms when the perturbation direction was known while t_{APA} was 60 ±15.93 ms when the perturbation was unknown (effect of *Condition*, $F_{(1,10)} = 26.05$, $p < 0.001$). There was no effect of perturbation direction on t_{APA} and no *Condition* × *Direction* interaction. The upper panel in **Figure 3.3** and Table 3.2 show the averages and standard error values for t_{APA} across the four conditions.

	BKn	FKn	BUn	FUn
t_{APA} (ms)	-113.18 ± 18.64	-121.09 ± 17.15	-70.36 ± 16.19	-49.64 ± 15.79

Table 3.2: Characteristics of APAs. The timing of APA (t_{APA}) are shown (means ± SE). R- and C-indices are in normalized units. BKn – backward perturbation with known direction; FKn – forward perturbation with known direction; BUn – backward perturbation with unknown direction; FUn – forward perturbation with unknown direction

In addition, under the Un conditions, subjects frequently showed unidirectional changes in the EMG levels within agonist-antagonist pairs during APAs. Note the increase in the activation level of both dorsal (SOL, BF and ESL) and ventral (TA, RF, and RA) muscles prior to the perturbation time ($t_0 = 0$) in **Figure 3.2**.

Table 3.3 presents the indices of APA activity ($\int$APA) values for all muscles averaged across subjects with standard errors for each of the four conditions. MANOVA showed a significant Condition × Direction interaction [$F_{(13,28)} = 3.140$, $p < 0.01$; Wilks' $\Lambda = 0.407$] without other effects (effect of Direction was close to

significance, p = 0.081). ANOVAs performed on individual muscle indices confirmed significant Condition × Direction interactions for TA, SOL, GM, GL, BF, ST, EST, and ESL ($p < 0.05$). Direction effects were significant for SOL, GM, ST, EST, and ESL, while Condition effects were significant for SOL, RF, EST, and ESL.

	BKn	FKn	BUn	FUn
TA	-0.008 ± 0.011	0.104 ± 0.032	0.114 ± 0.042	0.071 ± 0.023
SOL	-0.067 ± 0.024	0.1 ± 0.027	0.107 ± 0.03	0.056 ± 0.023
GM	-0.184 ± 0.059	0.133 ± 0.033	0.094 ± 0.061	0.009 ± 0.052
GL	-0.117 ± 0.07	0.189 ± 0.085	0.177 ± 0.073	0.059 ± 0.021
BF	-0.104 ± 0.027	0.119 ± 0.041	0.072 ± 0.047	0.007 ± 0.045
ST	-0.095 ± 0.029	0.147 ± 0.041	0.099 ± 0.045	0.058 ± 0.038
VL	0.018 ± 0.008	0.007 ± 0.009	0.01 ± 0.008	0.012 ± 0.012
RF	0.014 ± 0.009	-0.003 ± 0.011	-0.008 ± 0.01	-0.019 ± 0.007
VM	0.003 ± 0.006	-0.005 ± 0.009	0.022 ± 0.01	-0.002 ± 0.01
TFL	0.002 ± 0.006	0.033 ± 0.018	0.033 ± 0.021	0.007 ± 0.008
RA	0.003 ± 0.011	0.001 ± 0.011	0.002 ± 0.007	0.003 ± 0.006
EST	-0.113 ± 0.031	0.135 ± 0.024	0.102 ± 0.028	0.053 ± 0.026
ESL	-0.098 ± 0.021	0.128 ± 0.028	0.092 ± 0.024	0.034 ± 0.02
R-index	-1.024 ± 0.095	0.916 ± 0.118	0.616 ± 0.078	0.551 ± 0.151
C-index	0.091 ± 0.043	0.19 ± 0.056	0.384 ± 0.078	0.377 ± 0.09

Table 3.3: ∫APAs for individual muscles (∫EMGs activities during APAs), reciprocal (R-index), and co-activation (C-index) indices are shown (means ± SE). ∫APAs, R- and C-indices are in normalized units. BKn – backward perturbation with known direction; FKn – forward perturbation with known direction; BUn – backward perturbation with unknown direction; FUn – forward perturbation with unknown direction. See Table 3.1 for the abbreviation of muscles

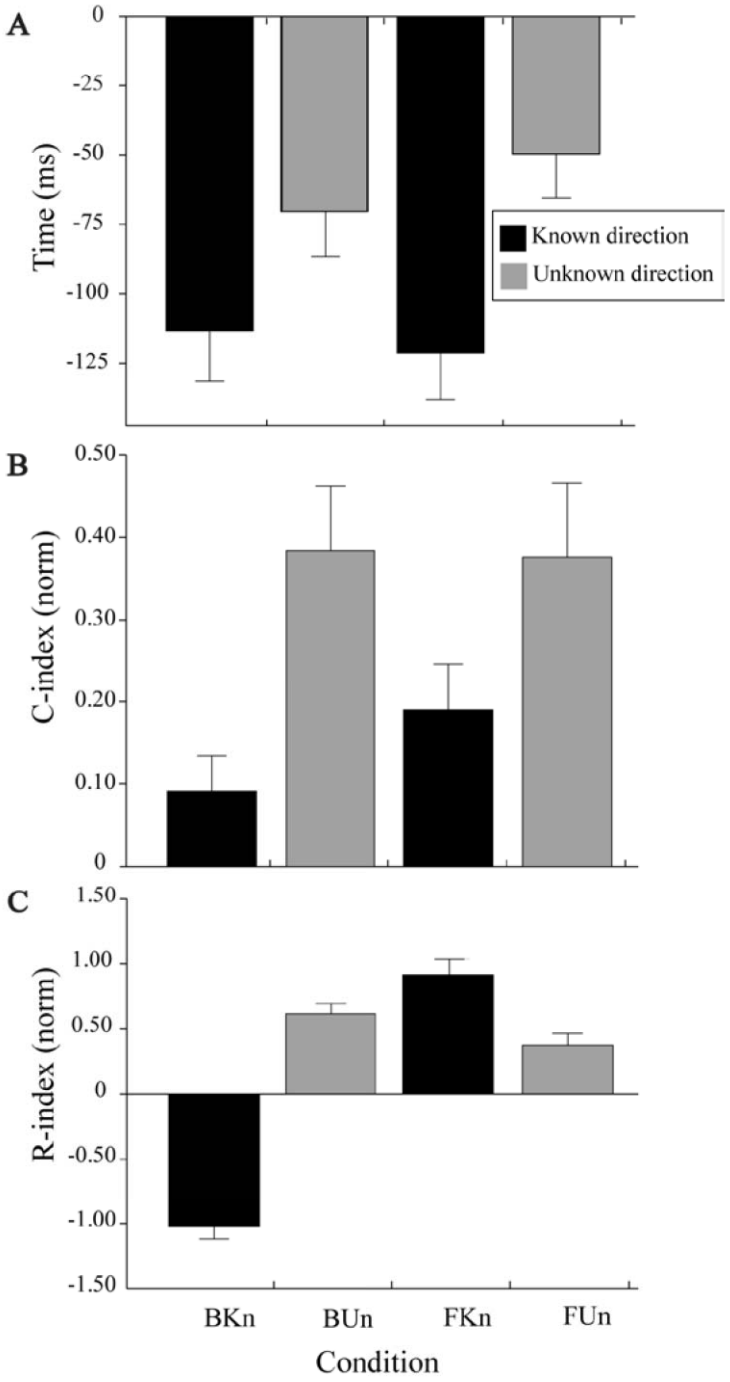

Figure 3.3: Averaged across subjects characteristics of anticipatory postural adjustments (APAs) are shown with standard error bars: (A) APA timing, tAPA; (B) C-index and (C) R-index. Note the significant delay in APAs (panel A) and the reorganization of APAs (panels B and C) when the perturbation direction was unknown (BUn and FUn). BKn – backward perturbation with known direction; FKn – forward perturbation with known direction; BUn – backward perturbation with unknown direction; FUn – forward perturbation with unknown direction

Further, we reduced the changes in individual muscle activations to two indices, the C-index and R-index, computed based on the M-mode values (see Methods) to quantify parallel vs. reciprocal changes in the EMG signals. These values are presented in Table 3.3 and in **Figure 3.3** (middle and lower panels).

Note the negative R-values for the BKn condition and positive values for the FKn condition. In contrast, for the BUn and FUn conditions, both values were positive and smaller in magnitude. These differences were reflected in significant effects of both Condition ($F_{(1,10)} = 87.77$, $p < 0.001$) and Direction ($F_{(1,10)} = 16.7$, $p < 0.01$), and a Condition × Direction interaction ($F_{(1,10)} = 78.37$, $p < 0.001$), with respect to the R-index. The interaction reflected the fact that Direction had a significant effect on the R-index when the subjects knew the perturbation direction ($p < 0.001$), while this was not true when the subjects did not know the perturbation direction. The C-index increased when the subjects had no prior knowledge about the direction of perturbation ($F_{(1,10)} = 9.1$, $p < 0.05$), without other effects.

3.3 Analysis of multi-M-mode synergies

We used the framework of the UCM hypothesis to quantify multi-M-mode synergies stabilizing the COP_{AP} trajectory. For this purpose, two components of variance in the M-mode space were quantified, V_{UCM} and V_{ORT} (see Methods). The time profiles of the averaged across subjects values of V_{UCM} and V_{ORT}, quantified per degree-of-freedom, are shown in **Figure 3.4** for each of the four conditions. Note the increase in V_{ORT} that could be seen about 200 ms prior to the perturbation time (t_0) across all conditions (shown with arrows in **Figure 3.4**).

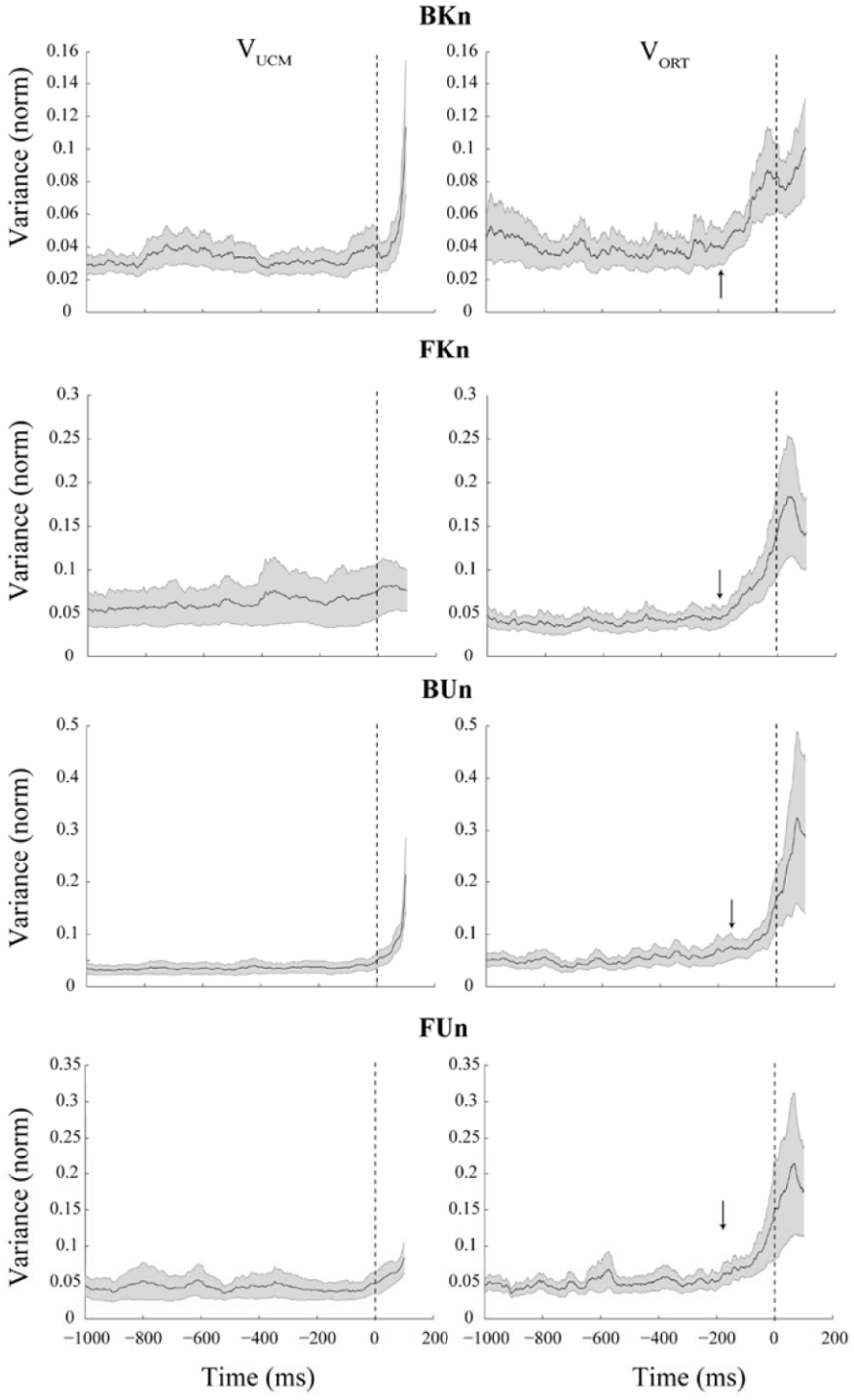

Figure 3.4: Time profiles of the two components of inter-trial variance, V_{UCM} (right plots) and V_{ORT} (left plot), averaged across subjects for each condition. The vertical dashed line corresponds to the onset of the perturbation (t_0=0). Note the similar time profile of V_{UCM} and V_{ORT} across the four condition and the increase of V_{ORT} before t_0 shown by arrows. BKn – backward perturbation with known direction; FKn – forward perturbation with known direction; BUn – backward perturbation with unknown direction; FUn – forward perturbation with unknown direction

These changes caused a drop in the synergy index (z-transformed, ΔV_Z), which we address as ASA. The time profiles of the synergy index during ASAs are illustrated in **Figure 3.5**. Averaged across subjects timing of ASAs with error bars is presented in **Figure 3.6** for the four conditions.

Note that the time of ASA initiation (t_{ASA}, shown with arrows in **Figure 3.5**) was seen prior to the initiation of APA (t_{APA}) across all four conditions. The averaged values of the changes in V_{UCM}, V_{ORT}, and ΔV_Z during ASAs (ΔV_{UCM}, ΔV_{ORT}, and $\Delta\Delta V_Z$, respectively) within each series are presented in Table 3.4.

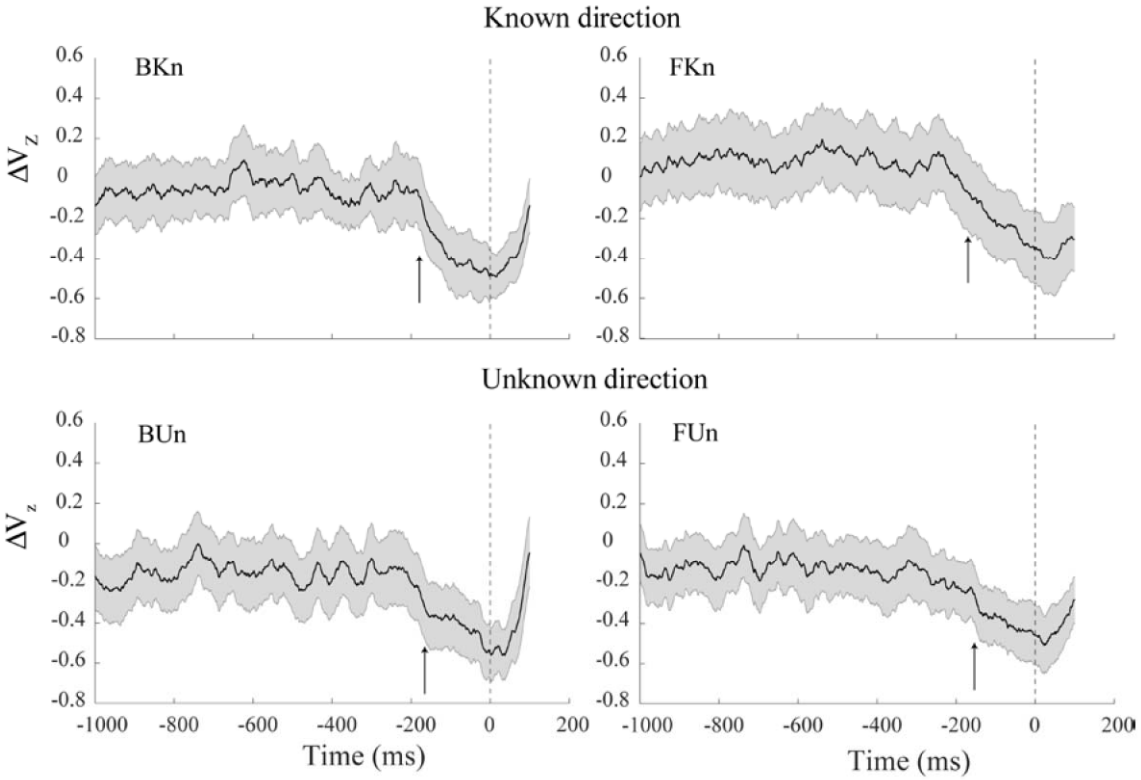

Figure 3.5: Time profiles of the synergy index (ΔV_Z), averaged across subjects for the four conditions. The vertical dashed line shows the perturbation time (t_0=0). The onset of ASAs initiation (t_{ASA}) is shown by arrows. Note the similar ΔV_Z values and time profiles across the four conditions. BKn – backward perturbation with known direction; FKn – forward perturbation with known direction; BUn – backward perturbation with unknown

	BKn	FKn	BUn	FUn
ΔV_{UCM}	-0.003 ± 0.005	-0.018 ± 0.011	-0.016 ±0.008	-0.005 ± 0.005
ΔV_{ORT}	-0.043 ± 0.012	-0.105 ± 0.044	-0.112 ± 0.048	-0.100 ± 0.053
$\Delta\Delta V_Z$	0.44 ± 0.04	0.46 ± 0.04	0.39 ± 0.07	0.38 ± 0.06

Table 3.4: Changes in the variance indices during ASAs. The means across subjects with standard error values are presented for the four conditions. ΔV_{UCM}, ΔV_{ORT}, $\Delta\Delta V_Z$ are in normalized units. BKn – backward perturbation with known direction; FKn – forward perturbation with known direction; BUn – backward perturbation with unknown direction; FUn – forward perturbation with unknown direction

During steady state, there were no significant effects of *Condition* and *Direction* on any of the three variance indices, V_{UCM}, V_{ORT}, and ΔV_Z (these values are presented in Table 3.4). ASA characteristics, the time of ASA initiation (t_{ASA}) and magnitude of the drop in the synergy index ($\Delta\Delta V_Z$), also showed no significant effects of these two factors. **Figure 3.6** depicts t_{ASA} data timing averaged across subjects for the four conditions. When the subject knew the perturbation direction in advance, t_{ASA} was 176.82 ± 13.81 ms (BKn) and 170.64 ± 8.32 ms (FKn), **Figure 3.6**. When the perturbation direction was unknown, t_{ASA} was 163.00 ±18.05 ms and 158.82 ± 22.17 ms for the BUn and FUn series, respectively.

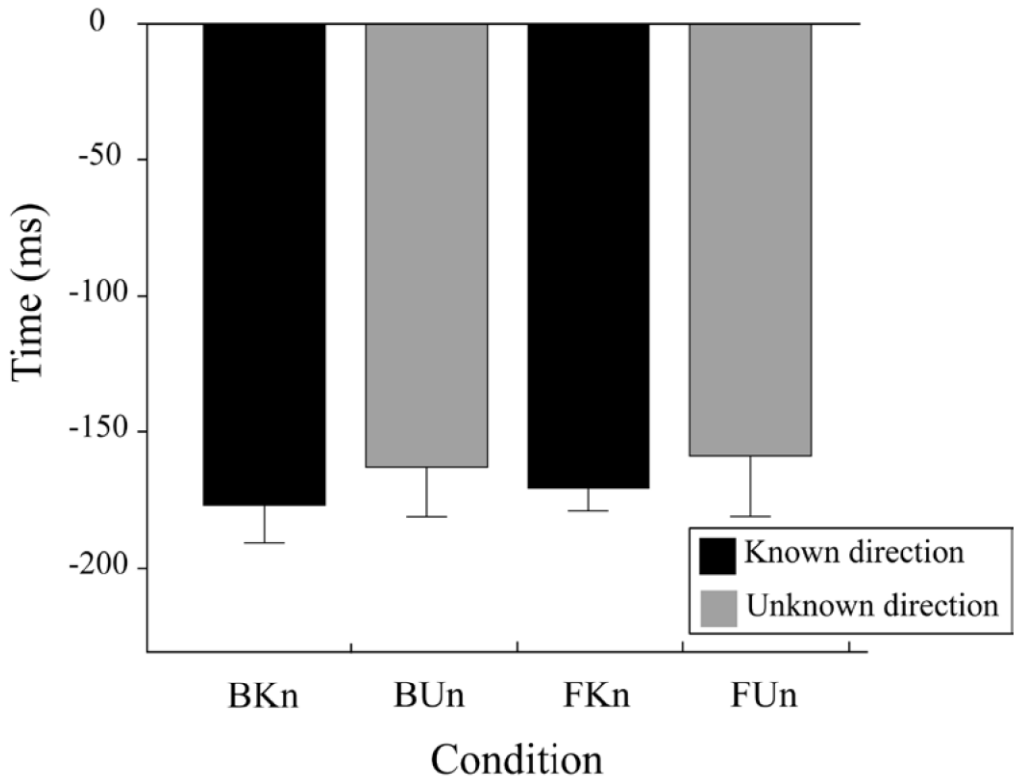

Figure 3.6: Characteristics of anticipatory synergy adjustments (ASAs) averaged across participants with standard error bars are shown for the four conditions. Note that ASAs occurred before APAs (see Figure 3.3). BKn – backward perturbation with known direction; FKn – forward perturbation with known direction; BUn – backward perturbation with unknown direction; FUn – forward perturbation with unknown direction

4 DISCUSSION

In the Introduction, we formulated contrasting predictions with respect to possible changes in anticipatory postural adjustments (APAs) and anticipatory synergy adjustments (ASAs) when the subjects become unable to predict direction of a self-triggered perturbation. Our observations provided support for all the specific hypotheses. In particular, we saw no significant changes in the two characteristics of ASAs (tASA and ΔΔVZ) between conditions with predictable and unpredictable direction of perturbations in support of Hypothesis 1. In contrast, there were significant changes in APA characteristics. In particular, as predicted by Hypothesis 2A, APAs became delayed under the conditions with unpredictable directions of perturbations. In addition, the typical reciprocal APA pattern observed when the subjects knew the direction of the perturbation in advance switched to a more pronounced co-contraction pattern in support of Hypothesis 2B. Overall, these results show that feed-forward control of vertical posture has two distinct components that depend differently on prior knowledge about perturbation direction. We discuss implications of these results for the recently proposed hierarchical scheme of the synergic control of motor tasks.

4.1 Multi-muscle synergies: Definitions and role in motor control

There is no consensus in the movement science literature on the meaning of synergy (reviewed in Latash and Zatsiorsky **2015**). In clinical studies, this word commonly means a stereotypical pattern of muscle activation interfering with purposeful voluntary movements seen commonly after stroke (Dewald et al. **1995**). More commonly, synergy means a group of variables with proportional involvement into an action over time and/or over changes in the action characteristics. In particular, synergies were defined as proportional changes in joint displacements, forces, and muscle activations (d'Avella et al. **2003;** Jerde et al. **2003;** Braido and Zhang **2004;** Zatsiorsky et al. **2004;** Tresch et al. **2006**). This definition emphasizes a reduction in the number of hypothetical variables manipulated by the controller as compared to the number of variables at the level of effectors. As such, synergies are supposed to contribute to dealing with the problem of motor redundancy.

A different definition has been formulated and developed recently based on the principle of motor abundance (Gelfand and Latash **1998;** Latash **2012**). This principle views the apparent excess of elemental variables at the level of effectors not as a source of computational problems for the neural controller but as a rich apparatus that can be used to provide stability of various performance variables in a task-specific way (Schöner **1995**). Synergies are defined in a space of elemental variables as neural organizations of the elemental variables with the purpose to stabilize task-specific salient variables.

Defining elemental variables is a non-trivial step in the definition and analysis of specific synergies (reviewed in Latash **2008**). In particular, during whole-body multi-

muscle tasks, stable muscle groups with proportional scaling of muscle activations have been viewed as elemental variables (M-modes, Krishnamoorthy et al. (**2003a**)); note that such groups are called synergies according to the second of the mentioned definitions.

According to the principle of motor abundance, the problem of motor redundancy is apparent, not real: The apparently redundant degrees-of-freedom are not eliminated but used in each trial in a flexible manner to ensure stable performance with respect to salient performance variables. The redundancy-abundance issue is discussed in detail in several recent reviews and books (Latash **2010;** Latash and Zatsiorsky **2015;** Latash **2016a**, **2016b**). Since we accept the principle of abundance, the arrangement of muscles into M-modes is not a step toward solving the problem of redundancy. Within the idea of movement control with changes in referent body configurations (RC hypothesis, (St-Onge and Feldman **2004;** Feldman **2011**, **2015**, **2016**)), M-modes may be viewed as reflections of elemental changes in the body RC, which are used as the basis for a variety of whole-body actions (Latash **2010**). This idea is indirectly supported by the analysis of whole-body actions as combinations of eigenmovements (Alexandrov et al. **2001**). An eigenmovement is movement along a new coordinate, which represents a linear combination of joint rotations; this coordinate is selected to ensure that movement along this coordinate depends only on the moment of force vector along the same coordinate and not on moments along other eigenmovements. The patterns of eigenmovements, analyzed both theoretically and experimentally, are compatible with changes in body configuration similar to

those addressed as ankle strategy and hip strategy, as well as with the typical composition of M-modes (Horak and Nashner **1986;** Robert et al. **2008**).

Note that the number of eigenmovements is not smaller than the number of joint rotations (both equal three in the studies of (Alexandrov et al. **2001**). This is an example of a more general idea that task-specific selection of a basis is not ruled by the idea of reducing the number of variables but by a deeper idea of ensuring an optimal basis given the control structure and task specificity. Such a change of the system of coordinates may reflect the nature of control with RCs. It may also be driven by the desire to use local control, i.e., changing an elemental variable only when that particular variable is perturbed. Using such control variables may be beneficial for implementing simple rule-based (algorithmic) control of the body able to ensure stability in conditions of unpredictable perturbations such as, for example, when slipping during walking on ice (Akulin et al. **2015**).

4.2 Feed-forward control of vertical posture

Mechanisms of feed-forward control of vertical posture were predicted by Bernstein (**1947**) and described for the first time about 50 years ago (Belen'kii et al. **1967**). Since those pioneering works, anticipatory postural adjustments have been studies vigorously in both young, healthy persons and populations with impaired postural control (reviewed in Massion **1992**, **1998**).

In particular, APA characteristics have been shown to depend on several factors such as properties of the perturbation (its magnitude, point of application, and direction), properties of action associated with the perturbation, time pressure, and stability of the initial posture (reviewed in Aruin **2002;** Latash and Hadders-Algra **2008**).

The purpose of APAs has been typically assumed as the generation of forces and moments directed against those expected from the perturbation(Cordo and Nashner **1982;** Bouisset and Zattara **1987;** Ramos and Stark **1990**). Note that, according to this hypothesis, APAs make functional sense only if the direction of forces/moments associated with a perturbation is known to the subject in advance. In our experiment, when this was not the case, APAs had to disappear or rearrange.

When properties of a perturbation are not known to the subject in advance, APAs show modifications compared to typical patterns seen when the subjects do not have to guess. In particular, when magnitude of a perturbation is unknown, subjects tend to generate APAs appropriate for the larger load (Aimola et al. **2011**) or scale them with respect to the load experienced in the immediately preceding trial (Toussaint et al. **1998**). To our knowledge, no previous studies explored APAs in conditions when direction of perturbation was unknown to the subject.

We observed two significant differences between the conditions with predictable and unpredictable perturbation directions: delayed APAs and prevalence of co-contraction patterns in agonist-antagonist muscle groups. Both changes may be seen as driven by safety considerations. Note that APAs have been shown to reverse their pattern and act in the direction of a self-triggered perturbation if their effects on COP shifts led the subject to a safer posture (Hirschfeld and Forssberg **1991;** Krishnamoorthy and Latash **2005**). In our study, APAs during the load manipulations were not vital for keeping vertical posture. COP shifts observed during APAs are relatively small in magnitude (on the order of a few mm (Bouisset and Zattara **1987;** Massion **1992**)) as compared to the distance from the edge of support. Indeed, when

similar tasks are performed in the simple reaction time paradigm, APAs are initiated closer to the moment of action initiation, and subjects have no problems keeping balance (Lee et al. **1987;** De Wolf et al. **1998**). However, even in the mentioned simple reaction time tasks, perturbation direction was always known to the subjects in advance.

Another strategy of APA adjustment in conditions viewed by the subjects as uncertain and/or otherwise difficult is to switch from the typical reciprocal pattern of muscle activation (optimal from the point of view of generating forces and moments) to an alternative pattern of co-contracting muscles. Note that co-contraction patterns during APAs have been described in the healthy elderly (Woollacott et al. **1988**), persons with atypical development (Aruin and Almeida **1997**), patients with neurological disorders (Asaka and Wang **2011**), as well as in young, healthy persons performing tasks associated with a difficult postural component (Gantchev and Dimitrova **1996**). In some of those conditions, even the organization of muscle into M-modes showed a switch from the typical patterns (e.g., similar to those illustrated in Table 3.1) to agonist-antagonist muscles represented in the same M-mode with loading factors of the same sign (co-contraction patterns (Asaka et al. **2008;** Danna-Dos-Santos et al. **2008**).

The significant changes in APA characteristics with predictability of the perturbation direction in our study stand in contrast to no changes in characteristics of the second feed-forward adjustment, ASAs. According to previous studies, the main purpose of ASAs is to reduce stability of a variable that the subject plans to change quickly (reviewed in Latash and Zatsiorsky **2015**). Indeed, producing a quick change in a

variable stabilized by a synergy requires overcoming one's own synergy. This is true independently of the planned direction of change in that variable. Indeed, an earlier study with known and unknown direction of changes in the force pulse produced by a set of fingers showed no dependence of ASAs on predictability of the force pulse direction (Zhou et al. **2013**).

To use a more intuitive example, when a goalkeeper gets ready for a penalty kick, he or she never stands perfectly quietly but shows substantial body sway, which may help to initiate the upcoming action independently of the direction of the kick. In clinical studies, a reduction in ASAs was seen in patients with Parkinson's disease who, according to the clinical examination, showed no signs of postural instability (Falaki et al. **2016**). It is possible that the inability to destabilize a variable with ASAs contributed to the well-known episodes of freezing, which represent one of the most disabling factors in these patients.

4.3 Feed-forward adjustments within hierarchical control

The notion of synergy fits naturally the hierarchical scheme for the control of movements developed recently (Latash **2010**, **2016a**). This scheme (**Figure 4.1**) is based on the idea of control with referent coordinates (RCs) for salient variables at each level of the hierarchy. At the highest level, a low-dimensional set of spatial RCs is used for the task-specific variables. Further, these variables undergo a chain of few-to-many transformations resulting in RCs at the level of elemental variables such as referent body configurations (reflected in M-modes), individual joint rotations, and ultimately, in RCs for the individual muscles. RCs at this latter level are equivalent to the values of the threshold of the tonic stretch reflex as in the classical equilibrium-

point hypothesis (Feldman **1966**, **1986**). Back-coupling loops ensure stability of values (time profiles) of RCs at higher levels by co-varied adjustments of RCs at lower levels (e.g., as in Latash et al. **2005**).

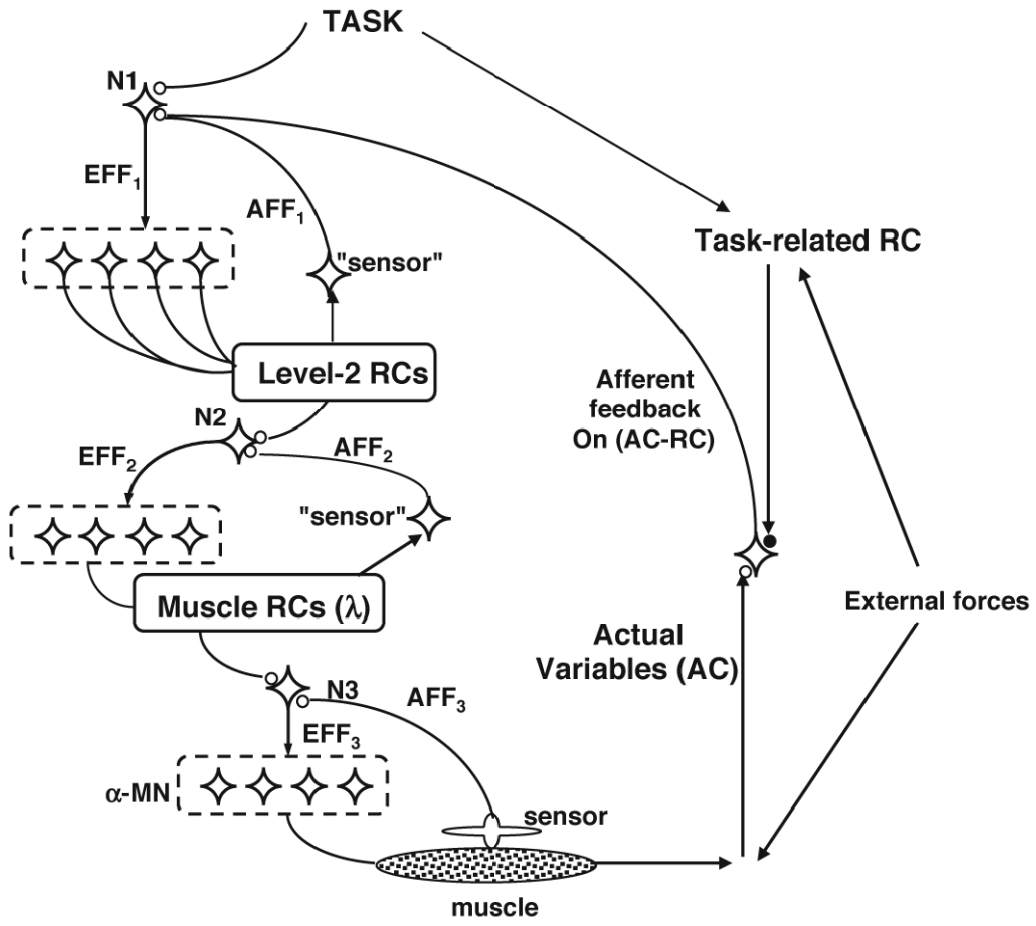

Figure 4.1: A scheme of a control hierarchy with referent configurations (RCs). The TASK defines an RC at the highest hierarchical level for a low-dimensional variable. Further, a sequence of few-to-many mappings leads to changes in tonic stretch reflex values (λ). for the involved muscles that drive the actual (Q) value to its referent value(R). Neural processes continue trying to minimize the difference between the actual and referent configurations at the task level, (AC–RC). Each level of the hypothetical scheme is organized in a synergic way with low-latency back-coupling loops (Latash et al. **2005**) based on afferent feedback (AFF) and efferent feed-forward signals (EFF). N – neurons; α-MN – α-motoneurons. From Zhou et al. (**2014**)

.

This scheme involves two types of neural variables that define target values (trajectories) for the salient variables and their stability properties, respectively. The former (NV1) are associated with the RCs at the task level, while the latter (NV2) may be associated with the gain matrix describing the back-coupling loops. The existence of these two classes of neural variables is supported by observations of unchanged performance with changes in synergy indices (e.g., during the ASAs, Olafsdottir et al. **2005;** Klous et al. **2011**), by changes in performance without changes in synergy indices (Friedman et al. **2009**), as well as by observations in neurological patients. In particular, patients with subcortical disorders, even at the earliest stages, typically demonstrate only slightly changed performance accompanied by significant changes in the synergy index (reviewed in Latash and Huang **2015**).

In contrast, patients after stroke sometimes demonstrate grossly changed performance with no changes in the synergy index (Reisman and Scholz **2003;** Jo et al. **2016b**).

These findings, taken together with the outcome of our study, are promising to increase the knowledge of salient features of the neural control of movement with potential implications for rehabilitation strategies. The theoretical framework of the concept of synergy and the hierarchical scheme for the control of movements need to be translated into rehabilitation science as they may help to develop new treatment strategies and approaches (reviewed in Piscitelli **2016**).

Feed-forward control of posture may be associated with changes in each group of the assumed neural variables. In particular, a change in NV1 in preparation to an action leads to APAs. In contrast, a change in NV2 leads to ASAs. Several earlier studies

have provided evidence for the different timing of ASAs and APAs in postural tasks (Klous et al. **2011;** Krishnan et al. **2011;** Krishnan et al. **2012**). ASAs emerge about 200-300 ms prior to the action initiation, while APAs start about 100 ms prior to the action initiation. This observation, by itself, also supports the idea of two groups of variables, NV1 and NV2, involved in the feed-forward control of tasks with postural components. Our results provide additional support for this scheme by showing decoupled changes in ASAs and APAs with changes in predictability of the perturbations.

A number of studies have provided evidence for parallel changes in features of ASAs and APAs. These include the delays in both adjustments under the simple reaction time instruction (De Wolf et al. **1998;** Olafsdottir et al. **2005**), delayed and reduced adjustments in the healthy elderly (Woollacott et al. **1988;** Olafsdottir et al. **2007**), and in certain patient groups (Bazalgette et al. **1986;** Park et al. **2012;** Jo et al. **2016b**). Since the neural processes leading to these two types of feed-forward adjustments are independent, at least hypothetically, the mentioned observations suggest that our understanding of the feed-forward processes is incomplete. There are likely higher-order processes involved in feed-forward control that are reflected in both ASAs and APAs, possibly related to a more general ability to anticipate forthcoming events(Klous et al. **2011;** reviewed in Latash and Zatsiorsky **2015**).

5 CONCLUSION

We have shown, for the first time, that two types of feed-forward control, reflected in APAs and ASAs, during motor tasks performed by standing persons show qualitatively different adjustments with changes in predictability of the direction of perturbation. These observations underscore the complexity of the feed-forward postural control, which involves separate changes in salient performance variables (such as COP coordinate) and in their stability properties. Preserved ASAs in conditions with unpredictable perturbation direction are functionally important because they destabilize the COP coordinate and facilitate later, corrective reactions to the actual perturbation. Note that the delayed and less efficient APAs make the corrective postural adjustments more important for keeping balance (cf. Santos et al. **2010;** Kanekar and Aruin **2014**).

5.1 Future directions

Neurorehabilitation can take advantage from the increased knowledge of these salient features of the neural control of movement as well as from the quantitative and objective measure of synergy index, which in some recent studies has been addressed as a preclinical marker for basal ganglia dysfunction (Falaki et al. **2016;** Lewis et al. **2016;** Falaki et al. **2017**).

Indeed, one of the significant problems in the field of neurorehabilitation is lack of objective evidence of clinical effectiveness of physiotherapy among patients with neurological impairments. There have been only a few definitive multi-site randomized clinical trials published over the last years (Dobkin et al. **2006;** Wolf et al.

2006; Lo et al. **2010;** Duncan et al. **2011;** Levy et al. **2016;** Winstein et al. **2016**). The majority of these trials (Dobkin et al. **2006;** Lo et al. **2010;** Duncan et al. **2011;** Levy et al. **2016;** Winstein et al. **2016**) reported negative results, i.e., no differences in the improvement in the primary outcome variables between the experimental and control group. Furthermore, recently Clarke et al. (**2016**) reported a clinic trial aiming to investigate the effectiveness of physiotherapy and occupational therapy in mild to moderate Parkinson disease revealing that the group receiving therapy did not show immediate or medium-term improvements in activities of daily living or quality of life. These disappointing outcomes could be due to the lack of translating the current theories of the neural control of movement into clinical and research settings. There is a clear need of translating the current theories on the neural control of movement into clinical research. Changes in the neural mechanisms of motor control have to be considered as an essential ingredient to guide and develop rehabilitation approaches.

So far, studies of synergies and stability of motor actions have been performed across several population of neurological patients including those with stroke, multi-system atrophy, multiple sclerosis, and Parkinson's disease (PD)(Latash and Huang **2015**). In recent studies on patients with early-stage PD, the synergy index and ASAs were both reduced compared to healthy matched subjects (Park et al. **2012;** Jo et al. **2015;** Jo et al. **2016a**). Interestingly, Falaki et al. (**2016**) found an impaired synergic control of posture in PD patients without clinical manifestations of postural instability. This was reflected in a significant reduced synergy indices during steady state, and significant reduced ASAs. The low synergy index reveals the low stability of steady-state actions in PD, while the inability to attenuate the synergy index prior to an action

could be causally related to the well-known clinical signs such as “freezing of gait” in PD.

Future researches should address how rehabilitation programs may benefit from the theoretical framework of hierarchical control with referent configuration and how physical therapy may improve impaired synergies that lead to poor control of movement stability.

6 REFERENCES

Aimola E, Santello M, La Grua G, Casabona A (2011) Anticipatory postural adjustments in reach-to-grasp: effect of object mass predictability. Neurosci Lett 502:84-88 doi: 10.1016/j.neulet.2011.07.027.

Akulin VM, Carlier F, Solnik S, Latash ML (2015) Neural Control of Redundant (Abundant) Systems as Algorithms Stabilizing Subspaces. arXiv preprint arXiv:1506.06920.

Alexandrov AV, Frolov AA, Massion J (2001) Biomechanical analysis of movement strategies in human forward trunk bending. I. Modeling. Biol Cybern 84:425-434 doi: 10.1007/PL00007986.

Aruin AS (2002) The organization of anticipatory postural adjustments. Journal of Automatic control 12:31-37.

Aruin AS (2003) The effect of changes in the body configuration on anticipatory postural adjustments. Motor Control 7:264-277.

Aruin AS, Almeida GL (1997) A coactivation strategy in anticipatory postural adjustments in persons with Down syndrome. Motor Control 1:178-191.

Aruin AS, Forrest WR, Latash ML (1998) Anticipatory postural adjustments in conditions of postural instability. Electroencephalogr Clin Neurophysiol 109:350-359.

Aruin AS, Latash ML (1995) Directional specificity of postural muscles in feed-forward postural reactions during fast voluntary arm movements. Exp Brain Res 103:323-332.

Asaka T, Wang Y (2011) Feedforward postural muscle modes and multi-mode coordination in mild cerebellar ataxia. Exp Brain Res 210:153-163 doi: 10.1007/s00221-011-2613-3.

Asaka T, Wang Y, Fukushima J, Latash ML (2008) Learning effects on muscle modes and multi-mode postural synergies. Exp Brain Res 184:323-338 doi: 10.1007/s00221-007-1101-2.

Asatryan DG, Feldman AG (1965) Functional tuning of the nervous system with control of movements or maintenance of a steady posture: I. Mechano-graphic analysis of the work of the joint on execution of a postural tasks. Biophysics 10:925–935.

Bazalgette D, Zattara M, Bathien N, Bouisset S, Rondot P (1986) Postural adjustments associated with rapid voluntary arm movements in patients with Parkinson's disease. Advances in neurology 45:371-374.

Belen'kii VE, Gurfinkel VS, Pal'tsev EI (1967) Control elements of voluntary movements. Biofizika 12:135-141.

Bernstein NA (1947) On the construction of movements. Medgiz, Moscow [in Russian].

Bernstein NA (1967) The co-ordination and regulation of movements. Pergamon Press, Oxford, New York.

Bouisset S, Zattara M (1987) Biomechanical study of the programming of anticipatory postural adjustments associated with voluntary movement. J Biomech 20:735-742.

Braido P, Zhang X (2004) Quantitative analysis of finger motion coordination in hand manipulative and gestic acts. Hum Mov Sci 22:661-678 doi: 10.1016/j.humov.2003.10.001.

Chen B, Lee YJ, Aruin AS (2015) Anticipatory and compensatory postural adjustments in conditions of body asymmetry induced by holding an object. Exp Brain Res 233:3087-3096 doi: 10.1007/s00221-015-4377-7.

Clarke CE, Patel S, Ives N, et al. (2016) Physiotherapy and Occupational Therapy vs No Therapy in Mild to Moderate Parkinson Disease: A Randomized Clinical Trial. JAMA Neurol:1-10 doi: 10.1001/jamaneurol.2015.4452.

Corcos DM, Gottlieb GL, Latash ML, Almeida GL, Agarwal GC (1992) Electromechanical delay: An experimental artifact. J Electromyogr Kinesiol 2:59-68 doi: 10.1016/1050-6411(92)90017-D.

Cordo PJ, Nashner LM (1982) Properties of postural adjustments associated with rapid arm movements. J Neurophysiol 47:287-302.

Cruse H, Bruwer M (1987) The human arm as a redundant manipulator: the control of path and joint angles. Biol Cybern 57:137-144.

d'Avella A, Saltiel P, Bizzi E (2003) Combinations of muscle synergies in the construction of a natural motor behavior. Nat Neurosci 6:300-308 doi: 10.1038/nn1010.

Danna-Dos-Santos A, Degani AM, Latash ML (2008) Flexible muscle modes and synergies in challenging whole-body tasks. Exp Brain Res 189:171-187 doi: 10.1007/s00221-008-1413-x.

Danna-Dos-Santos A, Slomka K, Zatsiorsky VM, Latash ML (2007) Muscle modes and synergies during voluntary body sway. Exp Brain Res 179:533-550 doi: 10.1007/s00221-006-0812-0.

De Wolf S, Slijper H, Latash ML (1998) Anticipatory postural adjustments during self-paced and reaction-time movements. Exp Brain Res 121:7-19.

Dewald JP, Pope PS, Given JD, Buchanan TS, Rymer WZ (1995) Abnormal muscle coactivation patterns during isometric torque generation at the elbow and shoulder in hemiparetic subjects. Brain 118 (Pt 2):495-510.

Dobkin B, Apple D, Barbeau H, et al. (2006) Weight-supported treadmill vs over-ground training for walking after acute incomplete SCI. Neurology 66:484-493 doi: 10.1212/01.wnl.0000202600.72018.39.

Duncan PW, Sullivan KJ, Behrman AL, et al. (2011) Body-weight-supported treadmill rehabilitation after stroke. N Engl J Med 364:2026-2036 doi: 10.1056/NEJMoa1010790.

Enderle JD, Wolfe JW (1987) Time-optimal control of saccadic eye movements. IEEE Trans Biomed Eng 34:43-55.

Falaki A, Huang X, Lewis MM, Latash ML (2016) Impaired synergic control of posture in Parkinson's patients without postural instability. Gait Posture 44:209-215 doi: 10.1016/j.gaitpost.2015.12.035.

Falaki A, Huang X, Lewis MM, Latash ML (2017) Dopaminergic modulation of multi-muscle synergies in postural tasks performed by patients with Parkinson's disease. J Electromyogr Kinesiol 33:20-26 doi: 10.1016/j.jelekin.2017.01.002.

Falaki A, Towhidkhah F, Zhou T, Latash ML (2014) Task-specific stability in muscle activation space during unintentional movements. Exp Brain Res 232:3645-3658 doi: 10.1007/s00221-014-4048-0.

Fedirchuk B, Dai Y (2004) Monoamines increase the excitability of spinal neurones in the neonatal rat by hyperpolarizing the threshold for action potential production. J Physiol 557:355-361 doi: 10.1113/jphysiol.2004.064022.

Feldman AG (1966) Functional tuning of the nervous system with control of movement or maintenance of a steady posture. II. Controllable parameters of the muscle. Biophysics 11:565–578.

Feldman AG (1980) Superposition of motor programs--I. Rhythmic forearm movements in man. Neuroscience 5:81-90.

Feldman AG (1986) Once more on the equilibrium-point hypothesis (lambda model) for motor control. J Mot Behav 18:17-54.

Feldman AG (2011) Space and time in the context of equilibrium-point theory. Wiley Interdiscip Rev Cogn Sci 2:287-304 doi: 10.1002/wcs.108.

Feldman AG (2015) Referent control of action and perception: challenging conventional theories in behavioral neuroscience. Springer, New York.

Feldman AG (2016) Active sensing without efference copy: referent control of perception. J Neurophysiol 116:960-976 doi: 10.1152/jn.00016.2016.

Feldman AG, Krasovsky T, Banina MC, Lamontagne A, Levin MF (2011) Changes in the referent body location and configuration may underlie human gait, as confirmed by findings of multi-muscle activity minimizations and phase resetting. Exp Brain Res 210:91-115 doi: 10.1007/s00221-011-2608-0.

Feldman AG, Levin MF (1995) Positional frames of reference in motor control: their origin and use. Behavioral and Brain Sciences 18:723–806 doi: 10.1017/S0140525X0004070X.

Feldman AG, Levin MF (2009) The equilibrium-point hypothesis--past, present and future. Adv Exp Med Biol 629:699-726 doi: 10.1007/978-0-387-77064-2_38.

Feldman AG, Orlovsky GN (1972) The influence of different descending systems on the tonic stretch reflex in the cat. Exp Neurol 37:481-494.

Flash T, Hogan N (1985) The coordination of arm movements: an experimentally confirmed mathematical model. J Neurosci 5:1688-1703.

Friedman J, Skm V, Zatsiorsky VM, Latash ML (2009) The sources of two components of variance: an example of multifinger cyclic force production tasks at different frequencies. Exp Brain Res 196:263-277 doi: 10.1007/s00221-009-1846-x.

Gantchev GN, Dimitrova DM (1996) Anticipatory postural adjustments associated with arm movements during balancing on unstable support surface. Int J Psychophysiol 22:117-122.

Gelfand IM, Latash ML (1998) On the problem of adequate language in motor control. Motor Control 2:306-313.

Gelfand IM, Tsetlin ML (1971) Some methods of controlling complex system. In: Gelfand IM, Gurfinkel VS, Fomin SV, Tsetlin ML (eds) Models of structural-functional organization of certain biological systems. MIT Press, Cambridge, MA, pp 329–345.

Gielen CC, Vrijenhoek EJ, Flash T, Neggers SF (1997) Arm position constraints during pointing and reaching in 3-D space. J Neurophysiol 78:660-673.

Glansdorf P, Prigogine I (1971) Thermodynamic Theory of Structures, Stability and Fluctuations. New York.

Hair JF, Anderson RE, Tatham RL, Black WC (1995) Factor analysis. In: Borkowski D (ed) Multivariate data analysis. Englewood Cliffs, Prentice Hall, pp 364-404.

Hasan Z (1986) Optimized movement trajectories and joint stiffness in unperturbed, inertially loaded movements. Biol Cybern 53:373-382.

Heckman CJ, Johnson M, Mottram C, Schuster J (2008) Persistent inward currents in spinal motoneurons and their influence on human motoneuron firing patterns. Neuroscientist 14:264-275 doi: 10.1177/1073858408314986.

Henneman E, Somjen G, Carpenter DO (1965) Excitability and inhibitability of motoneurons of different sizes. J Neurophysiol 28:599-620.

Hirschfeld H, Forssberg H (1991) Phase-dependent modulations of anticipatory postural activity during human locomotion. J Neurophysiol 66:12-19.

Horak FB, Nashner LM (1986) Central programming of postural movements: adaptation to altered support-surface configurations. J Neurophysiol 55:1369-1381.

Jackson JH (1889) On the comparative study of diseases of the nervous system. British Medical Journal 2:355-362.

Jerde TE, Soechting JF, Flanders M (2003) Coarticulation in fluent fingerspelling. J Neurosci 23:2383-2393.

Jo HJ, Ambike S, Lewis MM, Huang X, Latash ML (2016a) Finger force changes in the absence of visual feedback in patients with Parkinson's disease. Clin Neurophysiol 127:684-692 doi: 10.1016/j.clinph.2015.05.023.

Jo HJ, Maenza C, Good DC, Huang X, Park J, Sainburg RL, Latash ML (2016b) Effects of unilateral stroke on multi-finger synergies and their feed-forward adjustments. Neuroscience 319:194-205 doi: 10.1016/j.neuroscience.2016.01.054.

Jo HJ, Park J, Lewis MM, Huang X, Latash ML (2015) Prehension synergies and hand function in early-stage Parkinson's disease. Exp Brain Res 233:425-440 doi: 10.1007/s00221-014-4130-7.

Jobin A, Levin MF (2000) Regulation of stretch reflex threshold in elbow flexors in children with cerebral palsy: a new measure of spasticity. Dev Med Child Neurol 42:531-540.

Kanekar N, Aruin AS (2014) The effect of aging on anticipatory postural control. Exp Brain Res 232:1127-1136 doi: 10.1007/s00221-014-3822-3.

Kawato M (1999) Internal models for motor control and trajectory planning. Curr Opin Neurobiol 9:718-727.

Kelso JAS (1995) Dynamic patterns : the self-organization of brain and behavior. MIT Press, Cambridge, Mass.

Klous M, Danna-dos-Santos A, Latash ML (2010) Multi-muscle synergies in a dual postural task: evidence for the principle of superposition. Exp Brain Res 202:457-471 doi: 10.1007/s00221-009-2153-2.

Klous M, Mikulic P, Latash ML (2011) Two aspects of feedforward postural control: anticipatory postural adjustments and anticipatory synergy adjustments. J Neurophysiol 105:2275-2288 doi: 10.1152/jn.00665.2010.

Krawitz S, Fedirchuk B, Dai Y, Jordan LM, McCrea DA (2001) State-dependent hyperpolarization of voltage threshold enhances motoneurone excitability during fictive locomotion in the cat. J Physiol 532:271-281.

Krishnamoorthy V, Goodman S, Zatsiorsky V, Latash ML (2003a) Muscle synergies during shifts of the center of pressure by standing persons: identification of muscle modes. Biol Cybern 89:152-161 doi: 10.1007/s00422-003-0419-5.

Krishnamoorthy V, Latash ML (2005) Reversals of anticipatory postural adjustments during voluntary sway in humans. J Physiol 565:675-684 doi: 10.1113/jphysiol.2005.084772.

Krishnamoorthy V, Latash ML, Scholz JP, Zatsiorsky VM (2003b) Muscle synergies during shifts of the center of pressure by standing persons. Exp Brain Res 152:281-292 doi: 10.1007/s00221-003-1574-6.

Krishnan V, Aruin AS, Latash ML (2011) Two stages and three components of the postural preparation to action. Exp Brain Res 212:47-63 doi: 10.1007/s00221-011-2694-z.

Krishnan V, Latash ML, Aruin AS (2012) Early and late components of feed-forward postural adjustments to predictable perturbations. Clin Neurophysiol 123:1016-1026 doi: 10.1016/j.clinph.2011.09.014.

Latash ML (2000) There is no motor redundancy in human movements. There is motor abundance. Motor Control 4:259-260.

Latash ML (2008) Synergy. Oxford University Press, Oxford.

Latash ML (2010) Motor synergies and the equilibrium-point hypothesis. Motor Control 14:294-322.

Latash ML (2012) The bliss (not the problem) of motor abundance (not redundancy). Exp Brain Res 217:1-5 doi: 10.1007/s00221-012-3000-4.

Latash ML (2016a) Biological Movement and Laws of Physics. Motor Control:1-29 doi: 10.1123/mc.2016-0016.

Latash ML (2016b) Towards physics of neural processes and behavior. Neurosci Biobehav Rev 69:136-146 doi: 10.1016/j.neubiorev.2016.08.005.

Latash ML, Hadders-Algra M (2008) What is posture and how is it controlled? Clinics in Developmental Medicine 3:3-21.

Latash ML, Huang X (2015) Neural control of movement stability: Lessons from studies of neurological patients. Neuroscience 301:39-48 doi: 10.1016/j.neuroscience.2015.05.075.

Latash ML, Scholz JF, Danion F, Schoner G (2001) Structure of motor variability in marginally redundant multifinger force production tasks. Exp Brain Res 141:153-165 doi: 10.1007/s002210100861.

Latash ML, Scholz JP, Schoner G (2007) Toward a new theory of motor synergies. Motor Control 11:276-308.

Latash ML, Shim JK, Smilga AV, Zatsiorsky VM (2005) A central back-coupling hypothesis on the organization of motor synergies: a physical metaphor and a neural model. Biol Cybern 92:186-191 doi: 10.1007/s00422-005-0548-0.

Latash ML, Zatsiorsky VM (1993) Joint stiffness: Myth or reality? Human movement science 12:653-692.

Latash ML, Zatsiorsky VM (2015) Biomechanics and motor control: defining central concepts. Academic Press, Amsterdam.

Lee WA, Buchanan TS, Rogers MW (1987) Effects of arm acceleration and behavioral conditions on the organization of postural adjustments during arm flexion. Exp Brain Res 66:257-270.

Lepelley MC, Thullier F, Koral J, Lestienne FG (2006) Muscle coordination in complex movements during Jete in skilled ballet dancers. Exp Brain Res 175:321-331 doi: 10.1007/s00221-006-0552-1.

Levin MF (2014) Deficits in spatial threshold control of muscle activation as a window for rehabilitation after brain injury. Adv Exp Med Biol 826:229-249 doi: 10.1007/978-1-4939-1338-1_14.

Levin MF, Selles RW, Verheul MH, Meijer OG (2000) Deficits in the coordination of agonist and antagonist muscles in stroke patients: implications for normal motor control. Brain Res 853:352-369.

Levy RM, Harvey RL, Kissela BM, et al. (2016) Epidural Electrical Stimulation for Stroke Rehabilitation: Results of the Prospective, Multicenter, Randomized, Single-Blinded Everest Trial. Neurorehabil Neural Repair 30:107-119 doi: 10.1177/1545968315575613.

Lewis MM, Lee EY, Jo HJ, et al. (2016) Synergy as a new and sensitive marker of basal ganglia dysfunction: A study of asymptomatic welders. Neurotoxicology 56:76-85 doi: 10.1016/j.neuro.2016.06.016.

Lo AC, Guarino PD, Richards LG, et al. (2010) Robot-assisted therapy for long-term upper-limb impairment after stroke. N Engl J Med 362:1772-1783 doi: 10.1056/NEJMoa0911341.

Martin V, Scholz JP, Schoner G (2009) Redundancy, self-motion, and motor control. Neural Comput 21:1371-1414 doi: 10.1162/neco.2008.01-08-698.

Massion J (1992) Movement, posture and equilibrium: interaction and coordination. Prog Neurobiol 38:35-56.

Massion J (1998) Postural control systems in developmental perspective. Neurosci Biobehav Rev 22:465-472.

Matthews PB (1959) The dependence of tension upon extension in the stretch reflex of the soleus muscle of the decerebrate cat. J Physiol 147:521-546.

Mullick AA, Musampa NK, Feldman AG, Levin MF (2013) Stretch reflex spatial threshold measure discriminates between spasticity and rigidity. Clin Neurophysiol 124:740-751 doi: 10.1016/j.clinph.2012.10.008.

Musampa NK, Mathieu PA, Levin MF (2007) Relationship between stretch reflex thresholds and voluntary arm muscle activation in patients with spasticity. Exp Brain Res 181:579-593 doi: 10.1007/s00221-007-0956-6.

Olafsdottir H, Yoshida N, Zatsiorsky VM, Latash ML (2005) Anticipatory covariation of finger forces during self-paced and reaction time force production. Neurosci Lett 381:92-96 doi: 10.1016/j.neulet.2005.02.003.

Olafsdottir H, Zhang W, Zatsiorsky VM, Latash ML (2007) Age-related changes in multifinger synergies in accurate moment of force production tasks. J Appl Physiol (1985) 102:1490-1501 doi: 10.1152/japplphysiol.00966.2006.

Park J, Wu YH, Lewis MM, Huang X, Latash ML (2012) Changes in multifinger interaction and coordination in Parkinson's disease. J Neurophysiol 108:915-924 doi: 10.1152/jn.00043.2012.

Piscitelli D (2016) Motor rehabilitation should be based on knowledge of motor control. Archives of Physiotherapy 6:5 doi: 10.1186/s40945-016-0019-z.

Prilutsky BI, Zatsiorsky VM (2002) Optimization-based models of muscle coordination. Exerc Sport Sci Rev 30:32-38.

Ramos CF, Stark LW (1990) Postural maintenance during fast forward bending: a model simulation experiment determines the "reduced trajectory". Exp Brain Res 82:651-657.

Reisman DS, Scholz JP (2003) Aspects of joint coordination are preserved during pointing in persons with post-stroke hemiparesis. Brain 126:2510-2527 doi: 10.1093/brain/awg246.

Robert T, Zatsiorsky VM, Latash ML (2008) Multi-muscle synergies in an unusual postural task: quick shear force production. Exp Brain Res 187:237-253 doi: 10.1007/s00221-008-1299-7.

Rosenbaum DA, Meulenbroek RJ, Vaughan J, Jansen C (2001) Posture-based motion planning: applications to grasping. Psychol Rev 108:709-734.

Santos MJ, Kanekar N, Aruin AS (2010) The role of anticipatory postural adjustments in compensatory control of posture: 2. Biomechanical analysis. J Electromyogr Kinesiol 20:398-405 doi: 10.1016/j.jelekin.2010.01.002.

Schmidt RA (1975) A schema theory of discrete motor skill learning. Psychological review 82:225-260.

Schmitz C, Martin N, Assaiante C (2002) Building anticipatory postural adjustment during childhood: a kinematic and electromyographic analysis of unloading in children from 4 to 8 years of age. Exp Brain Res 142:354-364 doi: 10.1007/s00221-001-0910-y.

Scholz JP, Schoner G (1999) The uncontrolled manifold concept: identifying control variables for a functional task. Exp Brain Res 126:289-306.

Schöner G (1995) Recent developments and problems in human movement science and their conceptual implications. Ecological Psychology 8:291-314.

Shadmehr R, Wise SP (2005) The computational neurobiology of reaching and pointing: a foundation for motor learning. MIT Press, Cambridge, Mass.

Shim JK, Olafsdottir H, Zatsiorsky VM, Latash ML (2005) The emergence and disappearance of multi-digit synergies during force-production tasks. Exp Brain Res 164:260-270 doi: 10.1007/s00221-005-2248-3.

Slijper H, Latash ML (2000) The effects of instability and additional hand support on anticipatory postural adjustments in leg, trunk, and arm muscles during standing. Exp Brain Res 135:81-93.

Slijper H, Latash ML (2004) The effects of muscle vibration on anticipatory postural adjustments. Brain Res 1015:57-72 doi: 10.1016/j.brainres.2004.04.054.

Solnik S, Pazin N, Coelho CJ, Rosenbaum DA, Scholz JP, Zatsiorsky VM, Latash ML (2013) End-state comfort and joint configuration variance during reaching. Exp Brain Res 225:431-442 doi: 10.1007/s00221-012-3383-2.

St-Onge N, Feldman AG (2004) Referent configuration of the body: a global factor in the control of multiple skeletal muscles. Exp Brain Res 155:291-300 doi: 10.1007/s00221-003-1721-0.

Todorov E, Jordan MI (2002) Optimal feedback control as a theory of motor coordination. Nat Neurosci 5:1226-1235 doi: 10.1038/nn963.

Toussaint HM, Michies YM, Faber MN, Commissaris DA, van Dieen JH (1998) Scaling anticipatory postural adjustments dependent on confidence of load estimation in a bi-manual whole-body lifting task. Exp Brain Res 120:85-94.

Tresch MC, Cheung VC, d'Avella A (2006) Matrix factorization algorithms for the identification of muscle synergies: evaluation on simulated and experimental data sets. J Neurophysiol 95:2199-2212 doi: 10.1152/jn.00222.2005.

Turvey MT (1990) Coordination. Am Psychol 45:938-953.

Uno Y, Kawato M, Suzuki R (1989) Formation and control of optimal trajectory in human multijoint arm movement. Minimum torque-change model. Biol Cybern 61:89-101.

Winstein CJ, Wolf SL, Dromerick AW, et al. (2016) Effect of a Task-Oriented Rehabilitation Program on Upper Extremity Recovery Following Motor Stroke: The ICARE Randomized Clinical Trial. JAMA 315:571-581 doi: 10.1001/jama.2016.0276.

Winter DA, Prince F, Frank JS, Powell C, Zabjek KF (1996) Unified theory regarding A/P and M/L balance in quiet stance. J Neurophysiol 75:2334-2343.

Wolf SL, Winstein CJ, Miller JP, et al. (2006) Effect of constraint-induced movement therapy on upper extremity function 3 to 9 months after stroke: the EXCITE randomized clinical trial. JAMA 296:2095-2104 doi: 10.1001/jama.296.17.2095.

Wolpert DM, Ghahramani Z (2000) Computational principles of movement neuroscience. Nat Neurosci 3 Suppl:1212-1217 doi: 10.1038/81497.

Woollacott M, Inglin B, Manchester D (1988) Response preparation and posture control. Neuromuscular changes in the older adult. Ann N Y Acad Sci 515:42-53.

Zatsiorsky VM, Gao F, Latash ML (2005) Motor control goes beyond physics: differential effects of gravity and inertia on finger forces during manipulation of hand-held objects. Exp Brain Res 162:300-308 doi: 10.1007/s00221-004-2152-2.

Zatsiorsky VM, Latash ML, Gao F, Shim JK (2004) The principle of superposition in human prehension. Robotica 22:231-234 doi: 10.1017/S0263574703005344.

Zatsiorsky VM, Li ZM, Latash ML (1998) Coordinated force production in multi-finger tasks: finger interaction and neural network modeling. Biol Cybern 79:139-150 doi: 10.1007/s004220050466.

Zhou T, Solnik S, Wu YH, Latash ML (2014) Equifinality and its violations in a redundant system: control with referent configurations in a multi-joint positional task. Motor Control 18:405-424 doi: 10.1123/mc.2013-0105.

Zhou T, Wu YH, Bartsch A, Cuadra C, Zatsiorsky VM, Latash ML (2013) Anticipatory synergy adjustments: preparing a quick action in an unknown direction. Exp Brain Res 226:565-573 doi: 10.1007/s00221-013-3469-5.